

**3.3.1: Number of research papers published per teacher in the Journals as notified on UGC CARE list during the last five years**

3.3.1.1. Number of research papers in the Journals notified on UGC CARE list year wise during the last five years.

**CALENDAR YEAR 2022**

Title of paper	Name of the author/s	Department of the teacher	Name of journal	Calendar Year of publication	ISSN number	Link to the recognition in UGC enlistment of the Journal /Digital Object Identifier (doi) number		
						Link to website of the Journal	Link to article / paper / abstract of the article	Is it listed in UGC Care list
GENERALISED FIXED POINT THEOREMS IN FUZZY 2-METRIC SPACES	Dr. Shailesh Patel	Department of Humanities and Sciences	GIS SCIENCE JOURNAL	Nov-22	1869-9391	<a href="https://gissciencenet/">https://gissciencenet/</a>	<a href="https://drive.google.com/file/d/1PRDEbCqGULB6iSOsZRv4znRgC0mZZ3r9/view">https://drive.google.com/file/d/1PRDEbCqGULB6iSOsZRv4znRgC0mZZ3r9/view</a>	YES
Fixed point results in b-metric spaces over Banach algebra and contraction principle	Dr. Shailesh Patel	Department of Humanities and Sciences	GIS SCIENCE JOURNAL	Nov-22	1869-9391	<a href="https://gissciencenet/">https://gissciencenet/</a>	<a href="https://drive.google.com/file/d/1OV-tl8iVdA_Xir4ITCrCdef0tAuk7SRh/view">https://drive.google.com/file/d/1OV-tl8iVdA_Xir4ITCrCdef0tAuk7SRh/view</a>	YES

Title of paper	Name of the author/s	Department of the teacher	Name of journal	Calendar Year of publication	ISSN number	Link to the recognition in UGC enlistment of the Journal /Digital Object Identifier (doi) number		
						Link to website of the Journal	Link to article / paper / abstract of the article	Is it listed in UGC Care list
Effective Object Detection and Tracking for Holonomic Robot using Deep Neural Architecture	Prof. Hima Soni	Department of Electrical Engineering	IEEE	Jan-22	Electronic ISBN:978-1-6654-4175-9 Print on Demand(PoD) ISBN:978-1-6654-4176-6	<a href="https://ieeexplore.ieee.org/Xplore/home.jsp">https://ieeexplore.ieee.org/Xplore/home.jsp</a>	<a href="https://ieeexplore.ieee.org/document/9691596/">https://ieeexplore.ieee.org/document/9691596/</a>	Yes
Effective Object Detection and Tracking for Holonomic Robot using Deep Neural Architecture	Prof. Nirav Joshi	Department of Computer Engineering & Information Technology	INDICON-2021, IEEE Indicon, held at Indian Institute of Technology, Guwahati.	Jan-22	Electronic ISBN:978-1-6654-4175-9 Print on Demand(PoD) ISBN:978-1-6654-4176-6	<a href="https://ieeexplore.ieee.org/">https://ieeexplore.ieee.org/</a>	<a href="https://ieeexplore.ieee.org/document/9691596/">https://ieeexplore.ieee.org/document/9691596/</a>	Yes

## GENERALISED FIXED POINT THEOREMS IN FUZZY 2-METRIC SPACES

**SHEFAL H. VAGHELA, Dr. RITU KHANNA\*, Dr. SHAILESH T PATEL\*\***

**The Research Scholar of Pacific University, Udaipur (Rajasthan), India.**

**\*Professor Mathematics, Faculty of Engineering, Pacific University, Udaipur (Rajasthan), India.**

**\*\*S. P. B. Patel Engineering. College, Linch (Mehsana), India.**

**Abstract:** In this paper, we give some new extend, generalize and improve the corresponding results given by many authors compatible mappings of types -I & II in fuzzy-2 metric space prove.

**Keywords:** Fuzzy metric space, Compatible mappings, Common fixed point.

### 1. Introduction

Impact of fixed point theory in different branches of mathematics and its applications is immense. The first result on fixed points for contractive type mapping was the much celebrated Banach's contraction principle by S. Banach [10] in 1922. In the general setting of complete metric space, this theorem runs as the follows, Theorem 1.1(Banach's contraction principle) Let  $(X, d)$  be a complete metric space,  $c \in (0, 1)$  and  $f: X \rightarrow X$  be a mapping such that for each  $x, y \in X$ ,  $d(fx, fy) \leq c d(x, y)$  Then  $f$  has a unique fixed point  $a \in X$ , such that for each  $x \in X$ ,  $\lim_{n \rightarrow \infty} f^n x = a$ .

After the classical result, R.Kannan [11] gave a subsequently new contractive mapping to prove the fixed point theorem [12,13] & also in common [14] & 2-fuzzy [15,16]. Since then a number of mathematicians have been worked on fixed point theory dealing with mappings satisfying various type of contractive conditions. In 2002, A. Branciari [1] analyzed the existence of fixed point for mapping  $f$  defined on a complete metric space  $(X, d)$  satisfying a general contractive condition of integral type.

### 2 Preliminary Notes

**Definition 2.1** A binary operation  $*$  :  $[0,1] \times [0,1] \times [0,1] \rightarrow [0,1]$  is a continuous t-norms if  $([0,1], *)$  is an abelian topological monoid with unit 1 such that

$a_1 * b_1 * c_1 \leq a_2 * b_2 * c_2$  whenever  $a_1 \leq a_2$ ,  $b_1 \leq b_2$  and  $c_1 \leq c_2$   
for all  $a_1, a_2, b_1, b_2, c_1, c_2$  are in  $[0,1]$ .

**Definition 2.2** A 3-tuple  $(X, M, *)$  is said to be a fuzzy 2- metric space if  $X$  is an arbitrary set,  $*$  is a continuous t-norm and  $M$  is a fuzzy set on  $X^{3 \times} (0, \infty)$  satisfying the following conditions:

for all  $x, y, z, t \in X$  and  $t_1, t_2, t_3 > 0$ ,

- (1)  $M(x, y, z, t) > 0$ ;
- (2)  $M(x, y, z, t) = 1$ ,  $t > 0$  when at least two of the three points are equal
- (3)  $M(x, y, z, t) = M(x, z, y, t) = M(y, z, x, t)$
- (4)  $M(x, y, z, t_1) * M(x, u, z, t_2) * M(u, y, z, t_3) \leq M(x, y, z, t_1 + t_2 + t_3)$

The function value  $M(x, y, z, t)$  may be interpreted as the probability that the area of triangle is less than  $t$ .

(5)  $M(x, y, z, \cdot): [0,1] \rightarrow [0,1]$  is left continuous.

**Definition 2.3 [08]** Let  $(X, M, *)$  be a fuzzy- 2 metric space.

(1) A sequence  $\{x_n\}$  in fuzzy -2 metric space  $X$  is said to be convergent to a point  $x \in X$  (denoted by

$$\lim_{n \rightarrow \infty} x_n = x \text{ or } x_n \rightarrow x$$

if for any  $\lambda \in (0,1)$  and  $t > 0$ , there exists  $n_0 \in \mathbb{N}$  such that for all  $n \geq n_0$  and  $a \in X$ ,  $M(x_n, x, a, t) > 1 - \lambda$ .

That is

$$\lim_{n \rightarrow \infty} M(x_n, x, a, t) = 1 \text{ for all } a \in X \text{ and } t > 0.$$

(2) A sequence  $\{x_n\}$  in fuzzy- 2 metric space  $X$  is called a Cauchy sequence, if for any  $\lambda \in (0,1)$  and  $t > 0$ , there exists  $n_0 \in \mathbb{N}$  such that for all  $m, n \geq n_0$  and  $a \in X$ ,  $M(x_n, x_m, a, t) > 1 - \lambda$ .

(3) A fuzzy- 2 metric space in which every Cauchy sequence is convergent is said to be complete.

**Definition2.4 [08]** Self mappings  $A$  and  $B$  of a fuzzy- 2 metric space  $(X, M, *)$  is said to be compatible, if

$$\lim_{n \rightarrow \infty} M(ABx_n, BAx_n, a, t) = 1 \text{ for all } a \in X \text{ and } t > 0,$$

Whenever  $\{x_n\}$  is a sequence in  $X$  such that

$$\lim_{n \rightarrow \infty} Ax_n = \lim_{n \rightarrow \infty} Bx_n = z \text{ for some } z \in X. \text{ Then } \lim_{n \rightarrow \infty} ABx_n = Bz.$$

**Definition 2.5** Let  $(X, M, *)$  is a fuzzy-2 metric space. Then

(a) A sequence  $\{x_n\}$  in  $X$  is said to converse to  $x$  in  $X$  if for each  $\epsilon > 0$  and each  $t > 0$ ,  $\exists n_0 \in \mathbb{N}$  such

That  $M(x_n, x, t) > 1 - \epsilon$  for all  $n \geq n_0$ .

(b) a sequence  $\{x_n\}$  in  $X$  is said to Cauchy to if for each  $\epsilon > 0$  and each  $t > 0$ ,  $\exists n_0 \in \mathbb{N}$  such

That  $M(x_n, x_m, t) > 1 - \epsilon$  for all  $n, m \geq n_0$ .

(c) A fuzzy metric space in which every Cauchy sequence is convergent is said to be complete.

**Definition 2.6 [3]** Two self mappings  $f$  and  $g$  of a fuzzy metric space  $(X, M, *)$  are called compatible if

$$\lim_{n \rightarrow \infty} M(fgx_n, gfx_n, t) = 1 \text{ whenever } \{x_n\} \text{ is a sequence in } X \text{ such that } \lim_{n \rightarrow \infty} fx_n = \lim_{n \rightarrow \infty} gx_n = x$$

For some  $x$  in  $X$ .

**Definition 2.7 [1]**Two self mappings  $f$  and  $g$  of a fuzzy metric space  $(X, M, *)$  are called reciprocally continuous on  $X$  if  $\lim_{n \rightarrow \infty} fgx_n = fx$  and  $\lim_{n \rightarrow \infty} gfx_n = gx$  whenever  $\{x_n\}$  is a sequence in  $X$  such that

$$\lim_{n \rightarrow \infty} fx_n = \lim_{n \rightarrow \infty} gx_n = x \text{ for some } x \text{ in } X.$$

**Lemma 2.2.1[08]** Let  $(X, M, *)$  be a fuzzy- 2 metric space. If there exists  $q \in (0, 1)$  such that  $M(x, y, z, qt + 0) \geq M(x, y, z, t)$  for all  $x, y, z \in X$  with  $z \neq x, z \neq y$  and  $t > 0$ , then  $x = y$ ,

**Lemma 2.2.2[4]** Let  $X$  be a set,  $f, g$  owc self maps of  $X$ . If  $f$  and  $g$  have a unique point of coincidence,  $w = fx = gx$ , then  $w$  is the unique common fixed point of  $f$  and  $g$ .

### 3 Main Results

**Theorem 3.1**Let  $(X, M, *)$  be a complete fuzzy 2-metric space and let  $P, R, S$  and  $T$  be self-mappings of  $X$ . Let the pairs  $\{P, S\}$  and  $\{R, T\}$  be owc. If there exists  $q \in (0,1)$  such that

$$M(Px, Ry, a, qt) \geq \min \{M(Sx, Ty, a, t), M(Sx, Px, a, t), M(Ry, Ty, a, t), M(Px, Ty, a, t), M(Ry, Sx, a, t)\} \dots \dots \dots (1)$$

For all  $x, y \in X$  and for all  $t > 0$ , then there exists a unique point  $w \in X$  such that  $Pw = Sw = w$  and a unique point  $z \in X$  such that  $Rz = Tz = z$ . Moreover  $z = w$  so that there is a unique common fixed point of  $P, R, S$  and  $T$ .

**Proof :**Let the pairs  $\{P, S\}$  and  $\{R, T\}$  be owc, so there are points  $x, y \in X$  such that  $Px = Sx$  and  $Ry = Ty$ . We claim that  $Px = Ry$ . If not, by inequality (1)

$$\begin{aligned} M(Px, Ry, a, qt) &\geq \min \{ M(Sx, Ty, a, t), M(Sx, Px, a, t), M(Ry, Ty, a, t), M(Px, Ty, a, t), M(Ry, Sx, a, t) \} \\ &\geq \min \{ M(Px, Ry, a, t), M(Px, Px, a, t), M(Ty, Ty, a, t), M(Px, Ry, a, t), M(Ry, Px, a, t) \} \\ &\geq \min \{ M(Px, Ry, a, t), M(Px, Px, a, t), M(Ty, Ty, a, t), M(Px, Ry, a, t), M(Px, Ry, a, t) \} \\ &= M(Px, Ry, a, t). \end{aligned}$$

Therefore  $Px = Ry$ , i.e.  $Px = Sx = Ry = Ty$ . Suppose that there is another point  $z$  such that  $Pz = Sz$  then by (1) we have  $Pz = Sz = Ry = Ty$ , so  $Px = Pz$  and  $w = Px = Sx$  is the unique point of coincidence of  $P$  and  $S$ . By Lemma 2.8  $w$  is the only common fixed point of  $P$  and  $S$ . Similarly there is a unique point  $z \in X$  such that  $z = Rz = Tz$ .

Assume that  $w \neq z$ . we have

$$\begin{aligned} M(w,z,a,qt) &= M(Pw,Rz,a,qt) \\ &\geq \min \{ M(Sw,Tz,a,t), M(Sw,Pw,a,t), M(Rz,Tz,a,t), M(Pw,Tz,a,t), M(Rz,Sw,a,t) \} \\ &\geq \min \{ M(w,z,a,t), M(w,w,a,t), M(z,z,a,t), M(w,z,a,t), M(z,w,a,t) \} \\ &= M(w,z,a,t). \end{aligned}$$

Therefore we have  $z = w$  and  $z$  is a common fixed point of  $P, R, S$  and  $T$ . The uniqueness of the fixed point holds.

**Theorem 3.2** Let  $(X, M, *)$  be a complete fuzzy 2- metric space and let  $P, R, S$  and  $T$  be self-mappings of  $X$ . Let the pairs  $\{P,S\}$  and  $\{R,T\}$  be owc. If there exists  $q \in (0,1)$  such that

$$M(Px,Ry,a,qt) \geq \emptyset (\min \{ M(Sx,Ty,a,t), M(Sx,Px,a,t), M(Ry,Ty,a,t), M(Px,Ty,a,t), M(Ry,Sx,a,t) \}) \dots\dots\dots(2)$$

For all  $x, y \in X$  and  $\emptyset : [0,1] \rightarrow [0,1]$  such that  $\emptyset(t) > t$  for all  $0 < t < 1$ , then there exists a unique common fixed point of  $P, R, S$  and  $T$ .

**Proof :** Let the pairs  $\{P,S\}$  and  $\{R,T\}$  be owc, so there are points  $x, y \in X$  such that  $Px = Sx$  and  $Ry = Ty$ . We claim that  $Px = Ry$ . If not, by inequality (2)

$$\begin{aligned} M(Px,Ry,a,qt) &\geq \emptyset (\min \{ M(Sx,Ty,a,t), M(Sx,Px,a,t), M(Ry,Ty,a,t), M(Px,Ty,a,t), M(Ry,Sx,a,t) \}) \\ &> \emptyset (M(Px,Ry,a,t)). \quad \text{From Theorem 3.1} \\ &= M(Px,Ry,a,t). \end{aligned}$$

Assume that  $w \neq z$ . we have

$$\begin{aligned} M(w,z,a,qt) &= M(Pw,Rz,a,qt) \\ &\geq \emptyset (\min \{ M(Sw,Tz,a,t), M(Sw,Pw,a,t), M(Rz,Tz,a,t), M(Pw,Tz,a,t), M(Rz,Sw,a,t) \}) \\ &= M(w,z,a,t). \quad \text{From Theorem 3.1} \end{aligned}$$

Therefore we have  $z = w$  and  $z$  is a common fixed point of  $P, R, S$  and  $T$ . The uniqueness of the fixed point holds.

**Theorem 3.3** Let  $(X, M, *)$  be a complete fuzzy 2- metric space and let  $P, R, S$  and  $T$  be self-mappings of  $X$ . Let the pairs  $\{P,S\}$  and  $\{R,T\}$  be owc. If there exists  $q \in (0,1)$  such that

$$M(Px,Ry,a,qt) \geq \emptyset ( M(Sx,Ty,a,t), M(Sx,Px,a,t), M(Ry,Ty,a,t), M(Px,Ty,a,t), M(Ry,Sx,a,t)) \dots\dots\dots(3)$$

For all  $x, y \in X$  and  $\emptyset : [0,1]^7 \rightarrow [0,1]$  such that  $\emptyset(t,1,1,t,t,1) > t$  for all  $0 < t < 1$ , then there exists a unique common fixed point of  $P, R, S$  and  $T$ .

**Proof:** Let the pairs  $\{P,S\}$  and  $\{R,T\}$  be owc, so there are points  $x, y \in X$  such that  $Px = Sx$  and  $Ry = Ty$ . We claim that  $Px = Ry$ . If not, by inequality (3)

$$M(Px,Ry,a,qt) \geq \emptyset ( M(Sx,Ty,a,t), M(Sx,Px,a,t), M(Ry,Ty,a,t), M(Px,Ty,a,t), M(Ry,Sx,a,t))$$

$$\begin{aligned} &\geq \emptyset(M(Px,Ry,a,t), M(Px,Px,a,t), M(Ty,Ty,a,t), M(Px,Ry,a,t), M(Ry,Px,a,t)) \\ &\geq \emptyset( M(Px,Ry,a,t), M(Px,Px,a,t), M(Ty,Ty,a,t), M(Px,Ry,a,t),M(Px,Ry,a,t)) \\ &= \emptyset(M(Px,Ry,a,t), 1, 1, M(Px,Ry,a,t), M(Px,Ry,a,t)) \\ &=M(Px,Ry,a,t). \end{aligned}$$

A contradiction, therefore  $Px = Ry$ , i.e.  $Px = Sx = Ry = Ty$ . Suppose that there is a another point  $z$  such that  $Pz = Sz$  then by (3) we have  $Pz = Sz = Ry = Ty$ , so  $Px=Pz$  and  $w = Px = Sx$  is the unique point of coincidence of  $P$  and  $S$ .By Lemma 2.8  $w$  is the only common fixed point of  $P$  and  $S$ .Similarly there is a unique point  $z \in X$  such that  $z = Rz = Tz$ .Thus  $z$  is a common fixed point of  $P,R,S$  and  $T$ . The uniqueness of the fixed point holds from (3).

**Theorem 3.4** Let  $(X, M, *)$  be a complete fuzzy 2- metric space and let  $P,R,S$  and  $T$  be self-mappings of  $X$ . Let the pairs  $\{P,S\}$  and  $\{R,T\}$  be owc.If there exists  $q \in (0,1)$  for all  $x,y \in X$  and  $t > 0$

$$M(Px,Ry,a,qt) \geq M(Sx,Ty,a,t) * M(Sx,Px,a,t) * M(Ry,Ty,a,t) * M(Px,Ty,a,t) * M(Ry,Sx,a,t) \dots\dots\dots (4)$$

Then there exists a unique common fixed point of  $P,R,S$  and  $T$ .

**Proof:** Let the pairs  $\{P,S\}$  and  $\{R,T\}$  be owc, so there are points  $x,y \in X$  such that  $Px = Sx$  and  $Ry = Ty$ . We claim that  $Px = Ry$ . If not, by inequality (4)

We have

$$\begin{aligned} M(Px,Ry,a,qt) &\geq M(Sx,Ty,a,t) * M(Sx,Px,a,t) * M(Ry,Ty,a,t) * M(Px,Ty,a,t) * M(Ry,Sx,a,t) \\ &= M(Px,Ry,a,t) * M(Px,Px,a,t) * M(Ty,Ty,a,t) * M(Px,Ry,a,t) * M(Ry,Px,a,t) \\ &= M(Px,Ry,a,t) * 1 * 1 * M(Px,Ry,a,t) * M(Ry,Px,a,t) \\ &> M(Px,Ry,a,t). \end{aligned}$$

Thus we have  $Px = Ry$ , i.e.  $Px = Sx = Ry = Ty$ . Suppose that there is a another point  $z$  such that  $Pz = Sz$  then by (4) we have  $Pz = Sz = Ry = Ty$ , so  $Px=Pz$  and  $w = Px = Sx$  is the unique point of coincidence of  $P$  and  $S$ . Similarly there is a unique point  $z \in X$  such that  $z = Rz = Tz$ . Thus  $w$  is a common fixed point of  $P,R,S$  and  $T$ .

**Corollary 3.5** Let  $(X, M, *)$  be a complete fuzzy 2- metric space and let  $P,R,S$  and  $T$  be self-mappings of  $X$ . Let the pairs  $\{P,S\}$  and  $\{R,T\}$  be owc. If there exists  $q \in (0,1)$  for all  $x, y \in X$  and  $t > 0$

$$M(Px,Ry,a,qt) \geq M(Sx,Ty,a,t) * M(Sx,Px,a,t) * M(Ry,Ty,a,t) * M(Px,Ty,a,t) * M(Ry,Sx,a,2t) \dots\dots\dots(5)$$

Then there exists a unique common fixed point of  $P,R,S$  and  $T$ .

**Proof:** We have

$$\begin{aligned} M(Px,Ry,a,qt) &\geq M(Sx,Ty,a,t) * M(Sx,Px,a,t) * M(Ry,Ty,a,t) * M(Px,Ty,a,t) * M(Ry,Sx,a,2t) \\ &\geq M(Sx,Ty,a,t) * M(Sx,Px,a,t) * M(Ry,Ty,a,t) * M(Px,Ty,a,t) * M(Sx,Ty,a,t) \\ &\geq M(Sx,Ty,a,t) * M(Sx,Px,a,t) * M(Ry,Ty,a,t) * M(Px,Ty,a,t) * M(Px,Ry,a,t) \\ &= M(Px,Ry,a,t) * M(Px,Px,a,t) * M(Ty,Ty,a,t) * M(Px,Ry,a,t) * M(Ry,Px,a,t) \\ &= M(Px,Ry,a,t) * 1 * 1 * M(Px,Ry,a,t) * M(Ry,Px,a,t) \\ &>M(Px,Ry,a,t). \end{aligned}$$

And therefore from theorem 3.4,  $P, R, S$  and  $T$  have a common fixed point.

**Corollary 3.6** Let  $(X, M, *)$  be a complete fuzzy 2-metric space and let  $P,R,S$  and  $T$  be self-mappings of  $X$ . Let the pairs  $\{P,S\}$  and  $\{R,T\}$  be owc. If there exists  $q \in (0,1)$  for all  $x,y \in X$  and  $t > 0$

$$M(Px,Ry,a,qt) \geq M(Sx,Ty,a,t) \dots\dots\dots(6)$$

Then there exists a unique common fixed point of  $P,R,S$  and  $T$ .

**Proof:** The Proof follows from Corollary 3.5

**Theorem 3.7** Let  $(X, M, *)$  be a complete fuzzy 2- metric space.Then continuous self-mappings  $S$  and  $T$  of  $X$  have a common fixed point in  $X$  if and only if there exites a self mapping  $P$  of  $X$  such that the following conditions are satisfied

- (i)  $PX \subset TX \cap SX$
- (ii) The pairs  $\{P,S\}$  and  $\{P,T\}$  are weakly compatible,

(iii) There exists a point  $q \in (0, 1)$  such that for all  $x, y \in X$  and  $t > 0$   
 $M(Px, Py, a, qt) \geq M(Sx, Ty, a, t) * M(Sx, Px, a, t) * M(Py, Ty, a, t) * M(Px, Ty, a, t) * M(Py, Sx, a, t)$  .....(7)

Then P, S and T have a unique common fixed point.

**Proof:** Since compatible implies ows, the result follows from Theorem 3.4

**Theorem 3.8** Let  $(X, M, *)$  be a complete fuzzy 2- metric space and let P and R be self-mappings of X. Let the P and R are owc. If there exists  $q \in (0, 1)$  for all  $x, y \in X$  and  $t > 0$

$M(Sx, Sy, a, qt) \geq \alpha M(Px, Py, a, t) + \beta \min \{ M(Sx, Px, a, t), M(Sx, Py, a, t) \}$  .....(8)  
 For all  $x, y \in X$  where  $\alpha, \beta > 0, \alpha + \beta > 1$ . Then P and S have a unique common fixed point.

**Proof:** Let the pairs  $\{P, S\}$  be owc, so there are points  $x \in X$  such that  $Px = Sx$ . Suppose that exist another point  $y \in X$  for which  $Py = Sy$ . We claim that  $Sx = Sy$ . By inequality (8)

We have

$$\begin{aligned} M(Sx, Sy, a, qt) &\geq \alpha M(Px, Py, a, t) + \beta \min \{ M(Sx, Px, a, t), M(Sx, Py, a, t) \} \\ &= \alpha M(Sx, Sy, a, t) + \beta \min \{ M(Sx, Sx, a, t), M(Sx, Sy, a, t) \} \\ &= (\alpha + \beta) M(Sx, Sy, a, t) \end{aligned}$$

A contradiction, since  $(\alpha + \beta) > 1$ . Therefore  $Sx = Sy$ . Therefore  $Px = Py$  and Px is unique.  
 From lemma 2.2.2, P and S have a unique fixed point.

**Conclusion** It is also used in Fuzzy 3 metric spaces other type of metric. Also in integral metric spaces type in Fuzzy 2& 3 metric spaces

**References**

[1] A. Branciari. A fixed point theorem for mappings satisfying a general contractive condition of integral type. Int. J. Math. Sci. 29(2002), no.9, 531 - 536.

[2] A. George, P. Veeramani, "On some results in fuzzy metric spaces", Fuzzy Sets and Systems, 64 (1994), 395-399.

[3] Badard R. Fixed point theorems for fuzzy numbers. Fuzzy Set Syst 1984; 13:291–302.

[4] Bose BK, Sabani D. Fuzzy mappings and fixed point theorems. Fuzzy Set Syst 1987; 21-53.

[5] O. Kramosil and J. Michalek, "Fuzzy metric and statistical metric spaces", Kybernetika, 11 (1975), 326-334.

[6] B. Schweizer and A. Sklar, "Statistical metric spaces", Pacific J. Math. 10 (1960), 313-334.

[7] L.A. Zadeh, Fuzzy sets, Inform and Control 8 (1965), 338-353.

[8] Jinkyu Han. Common fixed point theorem on fuzzy-2 metric spaces. Int J Chung cheong Math Soci. 2010:302-729.

[9] M.S. Chauhan, Bharat Singh. Fixed point in intuitionistic fuzzy-3 metric space. Int. J. Engg and Techo. Vol.3 (2), 2011, 144-150.

[10]. S. Banach, Sur les opérations dans les ensembles abstraits et leur application aux équations intégrales, Fund. Math. 3, (1922) 133-181 (French).

[11] R. Kannan, Some results on fixed points, Bull. Calcutta Math. Soc., 60(1968), 71-76.

- [12] Jitendra Singhi, Ramakant Bhardwaj, Sarvesh Agrawal and Rajesh Shrivastava, “Fixed Point Theorem in Fuzzy Metric Spaces. “ International Mathematical Forum, 5, 2010, no. 30, 1473 – 1480.
- [13] K.S. Dersanambika, Aswathy M.R., “Fixed Point Theorems in Fuzzy Metric Spaces.” Int. J. Contemp. Math. Sciences, Vol. 6, 2011, no. 22, 1079 – 1089.
- [14] Namdeo Kailash, Shrivastav Rajesh, Solanki Manoj and Sharma Manoj4, “Common Fixed Point Theorem for four Mappings in Fuzzy Metric Space.” Research Journal of Mathematical and Statistical Sciences ISSN 2320–6047 Vol. 1(9), 11-14, October (2013).
- [15] R Krishnakumar and P Parakath Nisha Bagam, Fixed Point Theorems In Fuzzy 2-Metric Space With Implicit Map.” Int. J. Engg. Res. & Sci. & Tech. , ISSN 2319-5991, Vol. 3, No. 4, November 2014
- [16] R.Bhardwaj, S. Agrawal, Fixed Point Theorem in Fuzzy Metric Spaces, International Mathematical Forum, 5, 2010, no. 30, 1473 – 1480.

# Fixed point results in b-metric spaces over Banach algebra and contraction principle

SHEFAL H. VAGHELA, Dr. RITU KHANNA\*, Dr. SHAILESH T PATEL\*\*

The Research Scholar of Pacific University, Udaipur (Rajasthan), India.

\*Professor Mathematics, Faculty of Engineering, Pacific University, Udaipur (Rajasthan), India.

\*\*S. P. B. Patel Engineering. College, Linch (Mehsana), India.

## Abstract:

The main purpose of this paper is to present some fixed point results concerning the generalized contraction principle mappings in b-metric spaces over Banach algebras. We also give an example to support our main theorem. To obtain the results basic concept of fixed point that is Banach's contraction principle is mainly used and extension is obtained for various type of expressions. Obtained results are useful in image processing as well as in materials research for phase transition study and initial value and boundary value problems

**Keywords:** Fixed points; contraction type mapping; b-metric space; Banach algebras.

## 1. Introduction

The concept of b-metric space was introduced by Bakhtin [5] in 1989, which used it to prove a generalization of the Banach contraction principle in spaces endowed with such kind of metrics. Since then, this notion has been used by many authors to obtain various fixed point theorems. Aydi et al. in [4] proved common fixed point results for single valued and multi-valued mappings satisfying a weak  $\varphi$ -contraction in b-metric spaces. Roshan et al. in [19] used the notion of almost generalized contractive mappings in ordered complete b-metric spaces and established some fixed and common fixed point results. The concept of b-metric space coincides with the concept of metric space. For some details on subject see [7-20].

The aim of this paper is to generalize contraction principle mappings in b-metric spaces over Banach algebras and give an example to illustrate our main results.

## 2. Definitions Preliminaries

**Definition 2. 1.** ([11]) Let  $(X, d)$  be a nonempty set and  $s \geq 1$  be a given real number. A function  $d: X \times X \rightarrow [0, \infty)$  is a b-metric if, for all  $x, y, z \in X$ , the following conditions are satisfied:

$$(b1) \quad d(x, y) = 0 \text{ if and only if } x = y,$$

$$(b2) \quad d(x, y) = d(y, x),$$

$$(b3) \quad d(x, z) \leq s[d(x, y) + d(y, z)]$$

In this case, the pair  $(X, d)$  is called a b-metric space.

It should be noted that, the class of b-metric spaces is effectively larger than that of metric spaces; every metric is a b-metric with  $s = 1$ .

**Definition 2. 2.** ([10]) Let  $\{x_n\}$  be a sequence in a b-metric space  $(X, d)$ .

- a.  $\{x_n\}$  is called b-convergent if and only if there is  $x \in X$  such that  $d(x_n, x) \rightarrow 0$  as  $n \rightarrow \infty$ .
- b.  $\{x_n\}$  is a b-Cauchy sequence if and only if  $d(x_n, x_m) \rightarrow 0$  as  $n, m \rightarrow \infty$ .
- c. A b-metric space  $(X, d)$  is said to be complete if and only if each b-cauchy sequence in this space is b-convergent.

**Lemma 2. 3.** ([11]) Let  $(X, d)$  be a b-metric space with  $s \geq 1$ .

- i. If a sequence  $\{x_n\} \subset X$  is a b-convergent sequence, then it admits a unique limit.
- ii. Every b-convergent sequence in  $X$  is b-cauchy.

**Definition 2. 4.** ([10]) Let  $(X, d)$  be a b-metric space. A subset  $Y \subset X$  is called closed if and only if for each sequence  $\{x_n\}$  in  $Y$  which b-converges to an element  $x$ , we have  $x \in Y$ .

## 3. Main Results

**Definition 3. 1.** ([14]) Let  $X$  be a non empty set and  $\theta: X \times X \rightarrow [1, \infty)$ . A function  $d_\theta: X \times X \rightarrow [0, \infty)$  is called an extended b-metric if for all  $x, y, z \in X$  it satisfies:

$$d_\theta 1 \quad d_\theta(x, y) = 0 \text{ iff } x = y;$$

$$d_\theta 2 \quad d_\theta(x, y) = d_\theta(y, x);$$

$$d_{\theta}^3 d_{\theta}(x, z) \leq \theta(x, z)[d_{\theta}(x, y) + d_{\theta}(y, z)].$$

The pair  $(X, d_{\theta})$  is called an extended b-metric.

**Remark 3. 2.** If  $\theta(x, y) = s$  for  $s \geq 1$  then we obtain the definition of a b-metric space.

**Definition 3. 3.** ([14]) Let  $(X, d_{\theta})$  be an extended b-metric space.

- i. A sequence  $\{x_n\}$  in  $X$  is said to converge to  $x \in X$ , if for every  $\epsilon > 0$  there exists  $N = N(\epsilon) \in \mathbb{N}$  such that  $d_{\theta}(x_n, x) < \epsilon, \forall n \geq N$ . in this case, we write  $\lim_{n \rightarrow \infty} x_n = x$ .
- ii. A sequence  $\{x_n\}$  in  $X$  is said to be Cauchy, if for every  $\epsilon > 0$  there exists  $N = N(\epsilon) \in \mathbb{N}$  such that  $d_{\theta}(x_m, x_n) < \epsilon, \forall m, n \geq N$ .

**Definition 3. 4.** ([14]) An extended b-metric space  $(X, d_{\theta})$  is complete if every Cauchy sequence in  $X$  is convergent.

**Theorem 3. 5.** Let  $(X, d_{\theta})$  be a complete extended bms – basuch that  $d_{\theta}$  is a continuous functional with parameter  $s \geq 1$  and let the mappings  $T : X^2 \rightarrow X$  satisfying the contractive condition:

$$d_{\theta}(Tx, Ty) \leq k[d_{\theta}(x, Tx) + d_{\theta}(y, Ty) + d_{\theta}(x, y)] \forall x, y \in X, \quad (3.1)$$

Where  $k \in [0, 1)$  such that for each  $x \in X$ , Then  $T$  has a unique fixed point  $x \in X$  such that  $d_{\theta}(x, x) = 0$ .

**Proof:** Let  $x \in X$  From (3.1) we have

$$\begin{aligned} d_{\theta}(T^n x, T^{n+1} x) &\leq k d_{\theta}(T^{n-1} x, T^n x) \leq \dots \\ &\leq k^n d_{\theta}(x, Tx), \end{aligned} \quad (3.2)$$

Repeating this process we obtain

$$d_{\theta}(T^n x, T^{n+1} x) \leq k^n d_{\theta}(x, Tx), \quad (3.3)$$

Here the proof is divided into two cases:

**Case 1.**

Let  $T^n x = T^m x$  for some  $m, n \in \mathbb{N}, n \neq m$ . if  $m > n$  then  $T^{m-n}(T^n x) = T^n x$ , that is  $T^n x = y$ , where  $p = m - n$ . then

$$T^p y = y, \quad (3.4)$$

By (3.1) and (3.2), we have

$$d_\theta(y, Ty) = d_\theta(T^p y, T^{p+1} y) \leq k^p d_\theta(y, Ty) \quad (3.5)$$

Since  $k \in (0,1)$ , we get  $d_\theta(y, Ty) = 0$ , so  $y = Ty$ ; that is  $y$  is a fixed point of  $T$ .

### Case 2.

Suppose  $T^n x \neq T^m x, \forall m, n \in \mathbb{N}, n \neq m$ . we rewrite (3.2) as

$$\begin{aligned} & d_\theta(T^n x, T^{n+1} x) \\ & \leq s[k^n d_\theta(x, Tx)] \\ & \leq s[k^n d_\theta(x, Tx) + k^{n+1} d_\theta(x, Tx) + k^{n+2} d_\theta(x, Tx)] \\ & \leq s \sum_m^{\infty} s^m k^{n+m} (d_\theta(x, Tx)) \\ & \leq s \sum_m^{\infty} s^m k^m (d_\theta(x, Tx)) \end{aligned}$$

Since

$$d_\theta(T^n x, T^{n+m} x) \leq s \sum_m^{\infty} s^m k^m (d_\theta(x, Tx)) \quad (3.6)$$

Similarly, by (3.1), we have

$$\begin{aligned} d_\theta(T^n x, T^{n+2} x) & \leq k d_\theta(T^{n-1} x, T^{n+1} x) \leq \dots \\ & k^n d_\theta(x, T^2 x) \end{aligned}$$

$$\leq s \sum_m^{\infty} s^m k^{n+m} (d_{\theta}(x, Tx)) \quad (3.7)$$

For  $m > 3$  and  $m = 3p + 1, p \geq 1$  and using the fact that  $g^q x \neq g^r x, \forall q, r \in \mathbb{N}, q \neq r$ , we have

$$\begin{aligned} & d_{\theta}(T^n x, T^{n+m} x) \\ & \leq d_{\theta}(T^n x, T^{n+1} x) + s[d_{\theta}(T^{n+1} x, T^{n+2} x) + \dots \\ & \quad + d_{\theta}(T^{n+2p} x, T^{n+2p+1} x)] \\ & \leq s[k^n d_{\theta}(x, Tx) + k^{n+1} d_{\theta}(x, Tx) + \dots \\ & \quad + k^{n+2p} d_{\theta}(x, Tx)] \\ & \leq s \sum_m^{\infty} s^m k^{n+m} (d_{\theta}(x, Tx)) \\ & \leq s \sum_m^{\infty} s^m k^m (d_{\theta}(x, Tx)) \end{aligned}$$

Thus for  $m > n$  above inequality implies:

$$d_{\theta}(T^n x, T^{n+m} x) \leq s \sum_m^{\infty} s^m k^m (d_{\theta}(x, Tx))$$

Similarly, for  $m > 4$  and  $m = 3b + 2, b \geq 1$  and using the fact that  $g^q x \neq g^r x, \forall q, r \in \mathbb{N}, q \neq r$ ,

By triangular property, we have

$$\begin{aligned} & d_{\theta}(T^n x, T^{n+3b+2} x) \\ & \leq s[d_{\theta}(T^{n+3b+2} x, T^{n+3b+1} x) + d_{\theta}(T^{n+3b+1} x, T^{n+3b} x) + d_{\theta}(T^{n+3b} x, T^{n+3b-1} x) \\ & \quad + d_{\theta}(T^{n+3b-1} x, T^n x)] \end{aligned}$$

$$\begin{aligned}
&\leq s[d_{\theta}(T^n x, T^{n+1} x) + d_{\theta}(T^{n+1} x, T^{n+2} x) + \dots \dots \dots + d_{\theta}(T^{n+3b-1} x, T^{n+3b} x) \\
&\quad + d_{\theta}(T^{n+3b} x, T^{n+3b-1} x)] \\
&\leq s[k^n d_{\theta}(x, Tx) + k^{n+1} d_{\theta}(x, Tx) + \dots \dots \dots + k^{n+3b-1} d_{\theta}(x, Tx) + k^{n+3b} d_{\theta}(x, Tx)] \\
&\leq s \sum_m^{\infty} s^m k^{n+m} (d_{\theta}(x, Tx)) \\
&\leq s \sum_m^{\infty} s^m k^m (d_{\theta}(x, Tx))
\end{aligned}$$

Finally

$$d_{\theta}(T^n x, T^{n+m} x) \leq s \sum_m^{\infty} s^m k^m (d_{\theta}(x, Tx)) \quad (3.8)$$

We deduce from all cases that

$$d_{\theta}(T^n x, T^{n+m} x) \leq s[k^n d_{\theta}(x, T^2 x) + \frac{k^n}{1-k} d_{\theta}(x, Tx)] \quad \forall n, m \geq 0. \quad (3.9)$$

Therefore, we have

$$\lim_{n \rightarrow \infty} s d_{\theta}(T^n x, x) = \lim_{n \rightarrow \infty} s d_{\theta}(T^n x, T^m x) = d_{\theta}(x, x)$$

$$\text{Since } \lim_{n \rightarrow \infty} \frac{k^n}{1-k} s \|d_{\theta}(x, Tx)\| = 0$$

$$\text{We have } \lim_{n \rightarrow \infty} \|d_{\theta}(T^n x, T^{n+m} x)\| = 0, \quad \forall n, m \in \mathbb{N}$$

Which implies  $\{T^n x\}$ , is a Cauchy sequence in  $X$ .

By completeness of  $X$ , there exists  $u \in X$  such that

$$\lim_{n \rightarrow \infty} T^n x = u$$

Now we will show that  $u$  is a fixed point of  $T$  i.e.,  $Tu = u$ . without loss of generality, assume that  $T^k \neq u$  for any  $k \in \mathbb{N}$ . therefore the triangular inequality implies that

$$\begin{aligned}
& d_{\theta}(u, Tu) \\
& \leq s[d_{\theta}(u, T^n x) + d_{\theta}(T^n x, T^{n+1} x) + d_{\theta}(T^{n+1} x, Tu)] \\
& \leq d_{\theta}(u, T^n x) + s[d_{\theta}(T^n x, T^{n+1} x) + k[d_{\theta}(Tu, u) + d_{\theta}(T^n x, u)]] \\
& \Rightarrow d_{\theta}(u, Tu) \\
& \leq \frac{1}{1-k} s[d_{\theta}(u, T^n x) + d_{\theta}(T^n x, T^{n+1} x) + k d_{\theta}(T^n x, u)] \quad (3.10)
\end{aligned}$$

Taking limit as  $n \rightarrow \infty$ , and using (3.4) and (3.10), we have  $\|d_{\theta}(u, Tu)\| = 0$ .

Hence  $Tu = u$ . i. e.,  $u$  is a fixed point of  $T$ .

To show the uniqueness of fixed point  $u$ . suppose  $u^*$  is another fixed point of  $T$ , that is  $Tu^* = u^*$ .

Therefore,

$$d_{\theta}(u, u^*) = d_{\theta}(Tu, Tu^*) \leq k[d_{\theta}(u, Tu^*) + d_{\theta}(Tu, u^*) + d_{\theta}(u, u^*)] = 0$$

which implies that

$$\|d_{\theta}(u, Tu)\| = 0$$

That is,  $u = u^*$ . this completes the proof of the theorem.

**Example 3.2.** Let  $\mathcal{A} = \{a = (a_{ij})_{4 \times 4} : a_{ij} \in \mathbb{R}, 1 \leq i, j \leq 4\}$  and  $\|a\| = \frac{1}{4} \sum_{1 \leq i, j \leq 4} |a_{ij}|$ . Take  $P = \{a \in \mathcal{A} : a_{ij} \geq 0, 1 \leq i, j \leq 4\}$  in  $\mathcal{A}$ . Let  $X = \{1, 2, 3, 4\}$ .

Define a mapping  $d_{bms}: X^2 \times X \rightarrow \mathcal{A}$  by  $d(1,1) = d(2,2) = d(3,3) = d(4,4) = \theta$

$$d_{bms}(x, y) = \begin{cases} (2,1) \begin{pmatrix} 1,1,4,1 \\ 4,2,3,1 \\ 1,4,3,1 \\ 1,2,3,4 \end{pmatrix} & \text{if } x, y \in X; \\ (3,1) \begin{pmatrix} 4,1,4,1 \\ 4,3,5,2 \\ 2,3,1,4 \\ 3,4,2,1 \end{pmatrix} & \text{if } x, y \in X; \\ (4,1) \begin{pmatrix} 4,1,1,1 \\ 2,3,4,2 \\ 3,2,1,1 \\ 4,3,2,1 \end{pmatrix} & \text{if } x, y \in X; \\ (4,3) \begin{pmatrix} 16,9,12,7 \\ 20,8,6,2 \\ 9,8,4,4 \\ 16,12,9,4 \end{pmatrix} & \text{if } x, y \in X; \end{cases}$$

Then  $(X, d_{bms})$  is  $anbMS - BA$  over  $\mathcal{A}$  with coefficient  $p = \begin{pmatrix} 4,0,0,0 \\ 0,4,0,0 \\ 0,0,4,0 \\ 0,0,0,4 \end{pmatrix}$ .

## References

- [1] **Aamri, M. and Moutawakil, El. (2002)** ‘Some new common fixed point theorems under strict contractive conditions’, J. Math. Anal. Appl., 270, 181 – 188.
- [2] **Akkouchi, M. (2011)** ‘Common fixed point theorems for two self-mappings of a b-metric space under an implicit relation’, Hacet. J. Math. Stat., 40, 805{810.1

- [3] **Aydi, H. Bota, M. F., Karapinar, E., Moradi, S. (2012)** ‘A common fixed point for weak  $\emptyset$  – contractions on b-metric spaces’, Fixed Point Theory, 13, 337-346.
- [4] **Aydi, H., Felhi, A, and Sahmim, S. (2017)** Common fixed points via implicit contractions on b-metric like spaces. J. Nonlinear Sci Appl. 10, 1524-1537.
- [5] **Bakhtin, I. A. (1989)** ‘The contraction mapping principle in almost metric spaces’, Func. Anal., 30, 26{37.1, 1.1
- [6] **Beg, I., and Abbas, M. (2011)** ‘Coincidence and common fixed points of non-compatible maps’, J. Appl. Math. Inform., 29 743-752.1
- [7] **Boriceanu, M. (2009)** ‘Strict fixed point theorems for multi-valued operators in b-metric spaces’, Int. J. Mod. Math., 4 285-301.1, 1.3, 1.4
- [8] **Czerwik, S. (1993)** ‘Contraction mappings in b-metric spaces’, Acta Math. Inform. Univ. Ostraviensis, 1, 5{11.
- [9] **Demma, M., and Vetro, P. (2015)** ‘Picard sequence and fixed point results on b-metric spaces’, J. Function Spaces, 6 pages.
- [10] **Faraji, H.; Savić, D.; Radenović, S.(2019)**. Fixed point theorems for Geraghty contraction type mappings in b-metric spaces and applications. Axioms, 8, 34.
- [11] **Huang, S. and Xu, (2013)** Fixed point theorems of contractive mappings in cone b-metric spaces and applications’, Fixed Point Theory Appl., 10 pages.1
- [12] **Jungck, G. (1986)** ‘Compatible mappings and common fixed points’, Int. J. Math. Math. Sci., 9, 771{779.1.9
- [13] **Karapinar, E.; Czerwik, S.; Aydi, H. (2018)**.  $(\alpha, \gamma)$  –Meir-Keeler contraction mappings in generalized b-metric spaces. J. Funct. Spaces 3264620.
- [14] **Kamran, T. Samreen M., and Ain-Ul- Q. (2017)**.A Generalization of b-metric space and some fixed point Theorems, Mathematics MDPI, 5(19).
- [15] **Mudgal, S. (2014)** ‘Fixed Points Theorems for Weakly Compatible Maps along with Property (E.A.)’, International Journal of Computer Applications, 96(24), 0975-8887.
- [16] **Mlaiki, N. Kukic K., Filipovic, M., and Aydi. H. (2019)** On Almost b-metric spaces and Related Fixed point Results, Axioms 8(70), pp 1-12.

- [17] **Nazir, T., and Abbas, M. (2014)** ‘Common fixed points of two pairs of mappings satisfying (E.A)-property in partial metric spaces’, J. Inequal. Appl., 2014, 12 pages.1
- [18] **Ozturk, V., and Turkoglu, D. (2015)** ‘Common fixed point theorems for mappings satisfying (E:A)-property in b-metric spaces’, J. Nonlinear Sci. Appl., 8, 1127-1133.
- [19] **Ozturk, V., and Radenovi, S. (2016)** ‘Some remarks on b-(E.A)-property in b-metric spaces’, Springer Plus, 5, 544.
- [20] **Roshan, J. R., Parvaneh, V., and Altun, I., (2014)** ‘Some coincidence point results in ordered b-metric spaces and applications in a system of integral equations’, Appl. Math. Comput., 226, 725-737
- [21] **R. Bhardwaj and H.G. Sanath Kumar(2020)**, “B- Metric Space: An Application of Fixed Point”, Materials Today Proceedings, Vol 29, P2,659-663
- [22] **WadkarBalaji Raghunath, Ramakant Bhardwaj, Vishnu Narayan Mishra, Basant Kumar Singh(2017)** "Coupled Soft Fixed-Point Theorems in Soft Metric and Soft b- Metric Space", Scientific publications of the state university of Novi Pozar ser. A: appl. Math. Inform. And mech. vol. 9, No.1 59-73

# Effective Object Detection and Tracking for Holonomic Robot using Deep Neural Architecture

Atharva V. Pawar  
Computer Engineering Dept.  
Saffrony Institute of Technology  
Mehsana, India  
atharva.vijay.pawar@gmail.com

Sejal J. Rajput  
Computer Engineering Dept.  
Saffrony Institute of Technology  
Mehsana, India  
sejalrajput@gmail.com

Hima K. Soni  
Computer Engineering Dept.  
Saffrony Institute of Technology  
Mehsana, India  
hima.soni@saffrony.ac.in

Nirav R. Joshi  
Electrical Engineering Dept.  
Saffrony Institute of Technology  
Mehsana, India  
nirav.joshi@saffrony.ac.in

**Abstract**—The power of Deep Learning-based Computer Vision is not only making Object Detection tasks efficient but also more interesting. It gives an ability to computers for performing complex tasks as humans by locating and distinguishing between objects. The present research paper aims to create a robust tracking algorithm based on a custom-built dataset of a rugby ball, generated to replicate industrial objects. With the rapid growth in the automation industry, the need for compact yet reliable computational algorithms is a necessity. The primary objective behind the whole system is to achieve mobile compatibility with accurate object detection and tracking. The work also states the usage of the Convolutional Neural Networks (CNN) to increase the overall performance of pattern/image detection in tracking problems. A simple yet robust object tracking algorithm accompanied with object detection on Single Shot Multi-Box Detector (SSD) MobileNet architecture is applied in this paper. The method offers a minuscule model compatible to run on embedded systems without trading off much performance.

**Keywords**—Object Detection, Object Tracking, Holonomic Robot, Automation, Embedded System, Computer Vision

## I. INTRODUCTION

Object detection is an inextricable part of the modern field of computer vision [1]. The ability of computers to perform complex tasks to locate and distinguish between objects has disrupted the conventional method to pave the path towards the industrial revolution [2]. Defense, automobile, and security & surveillance are few among the many industries disrupted by advances in the field of object detection. Object tracking deals with estimating the trajectory of the object in a confined image plane [3]. A tracking algorithm uses object-centric information such as shape, color, bound area, and orientation of the object. Though an efficacious method to solve complex real-time problems, complex object shapes, inefficient 3D to the 2D projection of objects, noisy image, and real-time computational cost are hurdles for object tracking.

Autonomous systems in [4],[5] show the potential of combined systems to execute the tasks with human-like precision and if not, more. The amalgamation of object detection, object tracking, vision systems, and superior robotic maneuvering has led to more reliable systems. References [6],[7] outperforms the conventional drive of non-holonomy with the holonomic drive approach. Having a controllable degree of freedom equivalent to the total degree of freedom, the

holonomic drive is commonly used in several mobile robots to perform autonomous as well as semi-autonomous tasks.

Convolutional Neural Networks (CNN) offers excellent overall performance in pattern/image detection, surpassing human beings. Recent advances in CNN algorithms have opened new state-of-the-art techniques for image classification, object detection, object tracking, and semantic segmentation. Hierarchical feature representation has led to an increase in expressive capability and joint optimization [8], which surpasses the capabilities of traditional methods.

Various mobile robots were studied in [9],[10] dealing with, robot navigation, obstacle avoidance, and accelerated object tracking methods. The mobile robots had common characteristics of non-holonomic drive and constructed a framework based on CNN, fuzzy logic, image processing, or monocular vision feedback. The non-holonomic drive in the study showed less freedom for robust tracking of an object in the 2D plane, lacking in the continuous and proportional relationship between the speed of the object to be tracked with the speed of the robot.

Considering the scope of improvements in conventional methods of object tracking, a robust yet simple logical algorithm based on CNN to detect an object using the centroid of the bounding box is applied in this paper. The method offers a robust algorithm with freedom of locomotion on a horizontal plane with dynamic speed monitoring of the robot to locate, track, and follow. Also, the approach is tested on a holonomic robot accompanied with Omni wheels-based drive to evaluate the motion on the horizontal plane. The mechanical structure is monitored by an object detection model to detect rugby balls, trained on SSD MobileNet. This replicates the industrial application of tracking complicated objects. Also, providing a robust yet compact model to run on embedded systems.

## II. GENERIC OBJECT DETECTION AND TRACKING

Recent frameworks of object detection algorithms permit object classification and position estimation of detected objects. Moreover, the development of frameworks in [11],[12] overcome complexity such as occlusions, noisy images, information lost due to projection of environment into a 2D image, complex shapes of objects, and real-time computational requirements. These advances have helped make modern-day object detection algorithms more robust than ever.

In general object detection, once the object is detected, the tracking algorithm estimates the trajectory of the object through instance-by-instance evaluation of the frame in the video.

A flow and various approaches for object detection and tracking are demonstrated in Fig. 1.

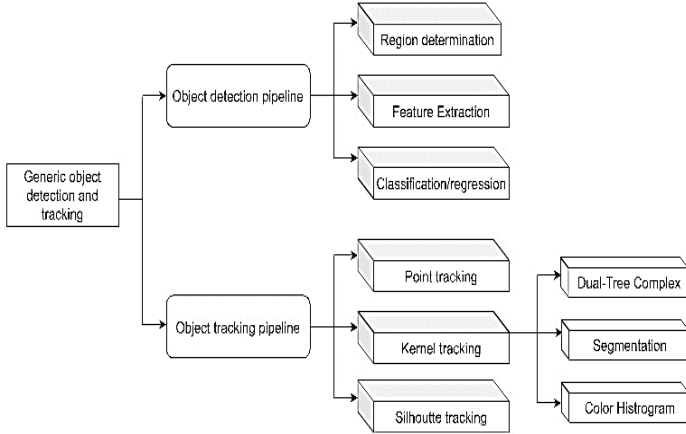


Fig. 1. Various object detection and tracking approaches

### A. Object detection pipeline

To determine the location of object (Object localization) and category of the detected object (Object classification), the pipeline of the object detection approach is divided into three stages which are further discussed below.

1) *Region determination*: Different classes of objects at multiple positions, different aspect ratios and sizes governs the computational expenses of the algorithm. Sliding multi-scale windows on images are observed to be an obvious yet exhaustive and inefficient method to locate the region of interest (ROI). Furthermore, work in [13] showcases the ability to mimic the human brain up to some extent for scanning and focusing on ROI by utilizing CNN into sliding window to directly predict the top-most feature (CNN layer) by bounding boxes after obtaining the confidence of the object class.

2) *Feature extraction*: To extract visual features, methods like segmentation, robust representation, and recognizing different classes are essential. These features are extracted from high dimensional features to final representation using CNN in a fixed resolution of the proposed region in the frame.

3) *Classification/ Regression*: Unique identification of the specific object's class is a vital parameter for the evaluation of models' robustness. More hierarchical, semantic, and informative visual recognitions presented using the classifier in [14] resulted in better clustering of classes. Utilizing CNN, allows the training of models to learn key representations without the need to design the features manually. The weights and biases in the network established are frozen to extract the best-performing model. Finally, different determined regions are scored on the set of positive regions (ROI) and negative regions (i.e., background). Bounding box regressors are then fit on the scored regions to extract the final location of the object.

### B. Object tracking pipeline

Continuous path estimation of the object in motion in the instance is the primary task of the object tracking algorithm. The target object is traced by selecting accurate features and object representations. In the first stage, optical flow, contours-based and histogram-based representation, and features recognized by CNN are some of the most common methods for feature detection. In the second stage, these feature detectors are utilized to create a correspondence between object occurrence in the frame both separately and jointly. Object tracking methods can be broadly categorized into three parts as discussed below.

1) *Point tracking*: The correspondence of detected objects is represented by points across the frames in point tracking. These points are identified using deterministic and statistical methods. Generic thresholding is done using point recognition. Moreover, occasions and false detections are shortcomings for the method.

2) *Kernel tracking*: Potential regions of objects are represented frame by frame for computing the object in motion. Parametric motions such as affined, conformal, and translational are observed. Usually, different types of objects are tracked, and approximating the motion of the object is done. Few kernel-based tracking approaches are:

a) *Dual-Tree Complex Wavelet Transform Technique*: Real wavelet transform employed here leads to poor directionality & shift variance and complex wavelet transform. Real filters are used to obtain shift variance in the tracking technique.

b) *Segmentation*: The approach finds the object in motion through optical flow computation. A considerable part of the video sequence is converted into gray-scale to apply the Horn-Schunk method for optical flow determination between any two images. The magnitude squared values of the optical flow,  $|V|^2$ , is calculated to compare the mean value of the first image with the optical flow of each pixel in the frame of the video sequence. Pixel values for each image are then set as true or high if  $|V|^2$ , at any pixel, is greater than or equal to the mean.

c) *Object tracking using Color Histogram*: Target model and candidate models are established in feature space to characterize the model. As illustrated in (1), the target model is defined as a probability density function  $\hat{q}$  in the given feature space. Similarly, the candidate model is defined as  $y$  and also characterized as the probability density function  $\hat{p}(y)$ . Further, a similarity function  $\hat{p}(y)$ , Bhattacharyya coefficient between  $\hat{p}$  and  $\hat{q}$  play the role of the likelihood for the local maxima in the frame indicating the presence of the object.

$$d(y) = \sqrt{1 - \rho[\hat{p}(y), \hat{q}]} \quad (1)$$

3) *Silhouette tracking*: Many times objects have complex shapes which cannot be fit geometrically in the object tracking mechanism, a silhouette-based approach is used to bound the detected objects in descriptive shapes. The method can represent in the form of edges, histogram, and contours. The silhouette tracking method can be classified into two categories, shape matching, and contour tracking.

### III. OBJECT DETECTION AND TRACKING USING ITERATIVE RE-CENTRING APPROACH

A robotic system was designed to implement the task of object detection and object tracking to capture the ball in motion with live feedback from vision systems.

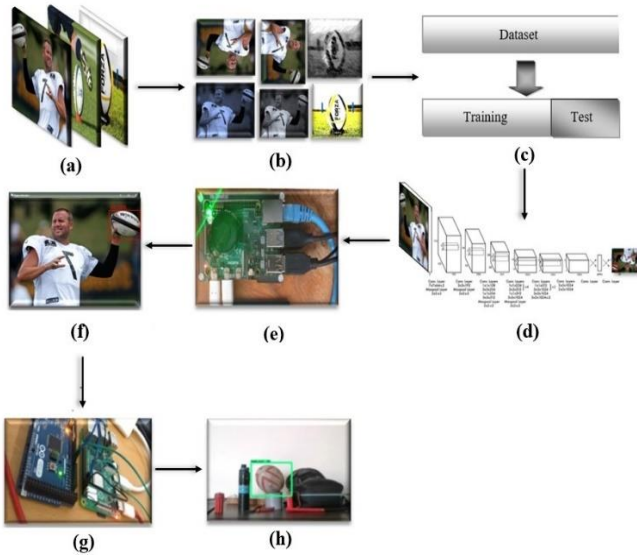


Fig. 2 (a) Gathering Images, (b) Augmentation, (c) Splitting Data, (d) Training of model, (e) Deploy on Raspberry Pi, (f) Run the model with bounding box and get coordinates, (g) Send coordinates to Arduino, (h) Track the ball.

To recognize the rugby ball distinctly, an object detection algorithm SSD MobileNet was utilized. The generated model by the algorithm being compact in terms of model size and computational power to run makes it feasible to accommodate it on an embedded system for the task of object detection. The steps performed and applied algorithms are demonstrated below:

#### A. Dataset

In object detection, images play a crucial role for a model to learn from and act as a source to gather salient features [15]. A total of 3300 sample images of rugby balls were collected in various orientations, backgrounds, colors, and angles. Such variance in sample images provides a generalized input for real possible scenarios while detection. Moreover, a close examination of the dataset was done to generate the same proportion of images with different characteristics to avoid undesirable bias for the model training.

The major portion of the dataset was gathered by employing the web-scraping algorithm to extract images of rugby balls effortlessly. The dataset also consisted of snaps of a rugby ball in different orientations, lighting conditions, and occlusions which were gathered locally. Finally, as shown in Fig. 2(a) all the images were resized to 300 X 300-pixel dimensions for equal scaling of all the data points.

#### B. Data augmentation and labeling

Due to the lack of ample amount of data points as well as the diversity of the data, inefficient extraction of salient features can be induced, resulting in underperformance of the model [16]. Data augmentation techniques applied on datapoints can

aid in scaling the dataset by folds and allows attaining the generalization by adding diversity to the data points. Data augmentation techniques such as interpolation, color distortion, blur, noise injection, cropping, flip, and rotations were applied as shown in Fig. 2(b).

The collected data points were split into training and testing data and annotated to provide the pivotal metadata for the supervised training of the model. Annotations are important features for determining the location and pixel area covered by the object in the image. Which helps in feature extraction while training, restricting computation to the ROI, and assists in robust modeling of the data points.

#### C. Model architecture and training

The images of the dataset were fine-tuned on a pre-trained neural architecture using the SSD algorithm, SSD MobileNet. The algorithm performs the tasks of object localization & classification, bounding box regression, and a classifier network to distinguish the detected objects. The architecture accompanies two deep neural networks, a base network (MobileNet) and a detection network (SSD). The base network can be divided into two blocks, depth-wise separable convolution ( $D_w$ ) and point-wise convolution ( $P_w$ ) [17].

*a) Depth-wise separable layer:* Depth-wise layer is utilized for filtering while the point-wise layer is utilized for combining the incoming feature maps from various channels. A standard convolutional layer consists of  $D_K \times D_K \times D_K$  input [17],  $M$  being the input channels through  $N$  convolution kernels for  $N$  feature maps for kernel size  $K$ . The standard computational cost can be calculated as in (2).

$$D_K \cdot D_K \cdot M \cdot N \cdot D_F \cdot D_F \quad (2)$$

$$D_K \cdot D_K \cdot M \cdot D_F + M \cdot N \cdot D_F \cdot D_F \quad (3)$$

Since a depth-wise separable convolution consists of depth-wise convolution and a point-wise convolution. The total computational cost is shown in (3). The computing ratio of depth-wise separable convolution and standard convolutions is expressed in (4).

$$\frac{D_K \cdot D_K \cdot M \cdot D_F \cdot D_F + M \cdot N \cdot D_F \cdot D_F}{D_K \cdot D_K \cdot M \cdot N \cdot D_F \cdot D_F} \quad (4)$$

A drastic decrement in the computation cost of depth-wise separable convolution can be learned in (5) [17].

$$\frac{1}{N} + \frac{1}{D_K^2} \quad (5)$$

*b) Inverted residuals:* The vulnerability of information loss increases after ReLU operation on lower-dimensional features in depth-wise separable convolution. The linear bottleneck is a complement to the depth-wise separable convolution. ReLU is replaced by a linear activation function to avoid further information losses. Point-wise convolution is used to advance the dimension to increase the channels after depth-wise processing.

*c) Single Shot MultiBox Detector (SSD):* The detection network is a single feed-forward-based convolutional neural

network capable of multi-target detection by simultaneously predicting the target categories with bounding boxes [18]. SSD is built on venerable VGG-16 architecture with six auxiliary feature layers, delivering strong performance in high-quality image classification and its ability to implement transfer learning to improve results. To predict the different types of offsets of the boxes with different scales, aspect ratios, and corresponding confidences, large amounts of multi-scaled borders are generated at different information layers. A fast class-agnostic bounding box co-ordinates proposal method is used for bounding box regression. The method uses a 1 X 1 convolution for dimensionality reductions but preserves the width and height. As in (6), the cumulative multi-box loss function is governed by confidence loss and location loss.

$$\text{multibox loss} = \text{confidence loss} + \alpha \times \text{location loss} \quad (6)$$

#### D. Tracking Algorithm

To track and maneuver the mechanism for rugby ball and get repeated feedback of the object in the environment through a vision system, a tracking algorithm was employed. The algorithm comes next in the pipeline after object detection in the frame as shown in Fig. 2(h). The frame is split into four quadrants and scaled for the input frame dimension of 480 X 360, resulting in diminishing the computational cost for frame evaluation. Moreover, the algorithm provides a tracking approach for the variable speed of the object in the frame. The centroid-focused tracking algorithm is divided into parts and explained:

a) *Generate bounding boxes*: The object in the frame is detected by the trained model. To generate the location of the detected rugby ball in the frame, rectangular bounding boxes are formed to enclose the target. Enabling accurate positioning of the rugby ball in the frame and aids in extracting the coordinates of the enclosed area in the rectangular space. The boxes can be generated in any quadrant of the frame leading to consistent locating.

b) *Generate centroid*: Though the bounding boxes can produce the accurate area of the rugby ball in the frame, they fail to extract the location of the object at point precision. Centroid-based tracking can solve the problem by calculating the centroid of the rectangular bounding box used to enclose the rugby ball for points  $M_{00}$ ,  $M_{01}$ ,  $M_{10}$ ,  $M_{11}$  as demonstrated in (7). Resulting in an average location of the detected object, returning a point on the X-Y plane. Diminishing the ROI into point of interest (POI), the task of precisely locating the object can be accomplished.

$$\frac{M_{00} + M_{01} + M_{10} + M_{11}}{4} \quad (7)$$

c) *Co-ordinate mapping and re-centering*: To track the motion of a rugby ball horizontally using an iterative re-centering mechanism, co-ordinate mapping is introduced. With the rugby ball in motion with variable velocity, the system can fail due to slow reaction time. Analog mapping of horizontal coordinates is implemented to assign variable speed for the horizontal re-centering of the robotic base. The positioning is monitored using iterative feedback from the vision system.

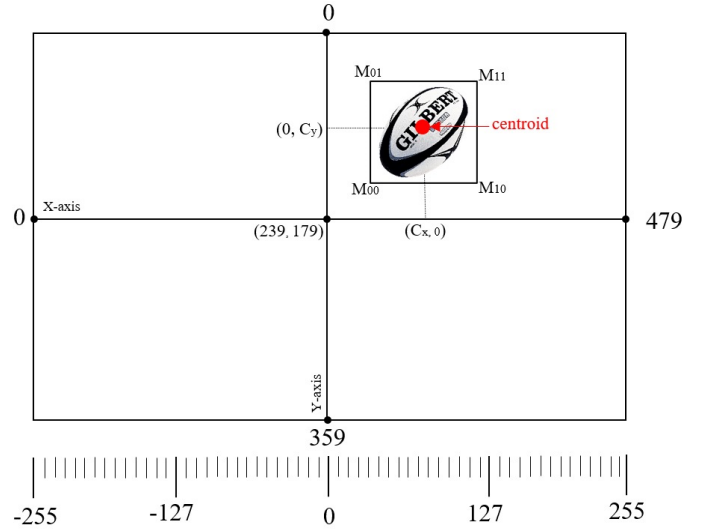


Fig. 3 Visualization of co-ordinate mapping and recentering

The base of the holonomic robot is dynamically re-centered for speed-sensitive to the horizontal coordinates of the detected centroid. The visualization of the iterative algorithm as depicted in Fig. 3 monitors in a simple yet robust manner and dynamically vary the velocity for tracking as well as re-centering the rugby ball.

#### IV. EXPERIMENTAL SETUP

The trained SSD MobileNet model and proposed object tracking method were tested on the holonomic structure shown in Fig. 4. The system includes four Omni-wheels coupled with planetary gear motors at the base providing smooth locomotion on a horizontal plane. This allows a degree of freedom for two axes. The structure incorporates a vision system, computational boards: Raspberry Pi, Arduino Mega, Motor Drivers to synchronize the motion of motors, and Communication Bus Architecture to regulate the transferring of information between computational boards. The system is powered by a 12V LiPo battery. Which supplies power to motor drivers, synchronizing the motors. The actions of these motor drivers are regulated by Arduino Mega assisted by logical conditions applied in Arduino sketch.

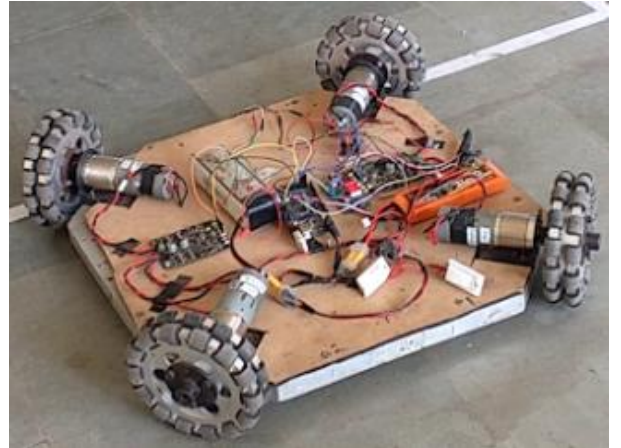


Fig. 4. Holonomic Structure

The camera module in connection with Raspberry Pi 4B with 4GB RAM and quad-core A72 cortex processor, captures the frames in the live feed. The captured frame is monitored to detect the rugby ball with bounding boxes. The coordinates of the detected bounding boxes are utilized to calculate centroid points and transferred to the Arduino Mega using the I2C communication protocol. The base of the robot is re-centered sensitively using analog-based velocity mapping under the monitoring of logical parameters by Arduino. The system was tested in multiple environments.

## V. RESULTS AND DISCUSSION

The paper presents the results of the validation of the rugby ball dataset. The dataset was split into a split ratio of 0.8 and 0.2 for the training and validation of the model, respectively. The model was trained up to 25100 iterations. For the overall evaluation of our approach, several evaluation metrics were performed to study the results.

### A. Evaluation of training performance

For detection of a rugby ball, the SSD MobileNet was fine-tuned on the custom dataset. The training session was conducted on Tesla K80 GPU with 12GB RAM. Based on the training session, various observations have been done using TensorBoard with step and their respective losses on the x-axis and y-axis respectively as shown in Fig. (5)-(9).

To evaluate the accuracy of the prediction of classes by model, classification loss as shown in Fig. 5 was plotted. With an increment in the number of steps, the losses decreased constantly till 0.2. This showcases the robust classification ability of the trained model.

The localization loss as shown in Fig. 7 was visualized to evaluate the error between predicted bounding box corrections and true values. The results show minimal losses due to localization resulting in a reduction of loss to 0.1. Moreover, Normalized loss in Fig. 7, as well as regularization loss in Fig. 8, were reduced below 0.5 and 0.2, respectively. This demonstrates the generalization property of the model, leading towards better accuracy.

Finally, the total loss in Fig. 9 was a plot for evaluating the overall loss in terms of classification, regularization, and localization. Total loss constantly decreased up to 0.5.

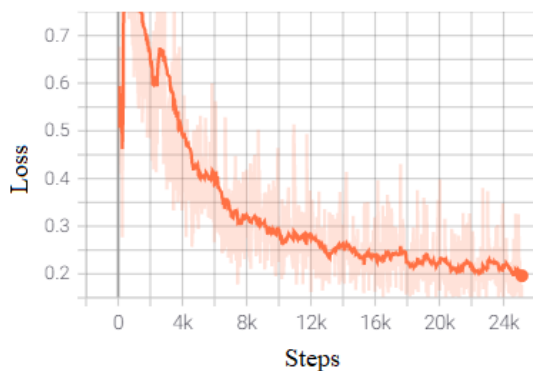


Fig. 5. Classification Loss

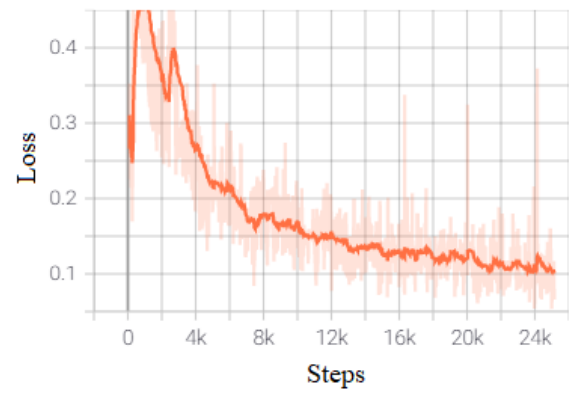


Fig. 6. Localization Loss

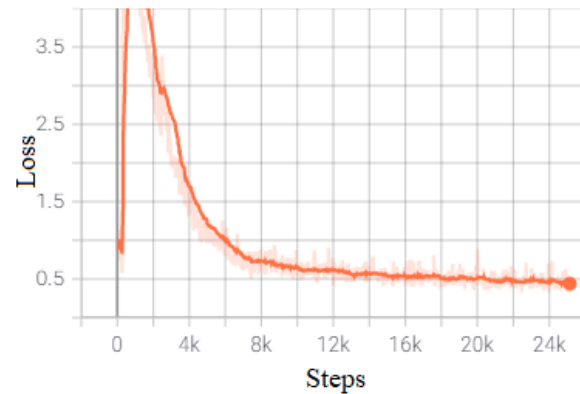


Fig. 7. Normalized Loss

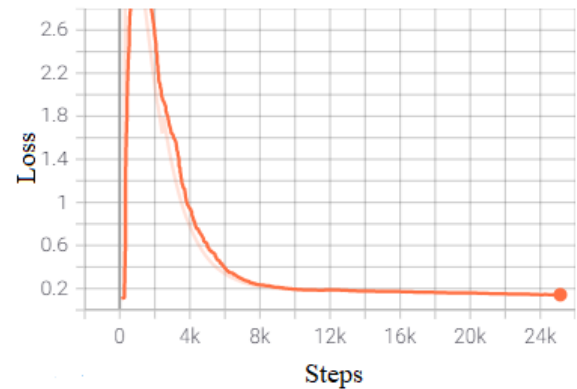


Fig. 8. Regularization Loss

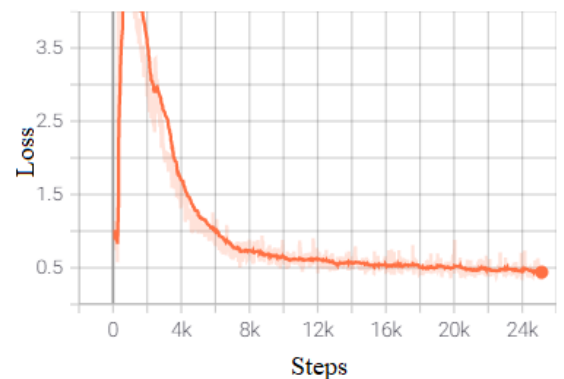


Fig. 9. Total Loss

## B. Object detection in action

After model training and studying the graphs, a minuscule model was tested to detect the rugby ball in various robust environments along with multiple objects in the surroundings. Moreover, to test the reliability of the generalization of the trained model, the rugby ball was adjusted at different orientations. As seen in Fig. 10 the model was able to detect the location of the rugby ball at different orientations and could distinguish between different objects.

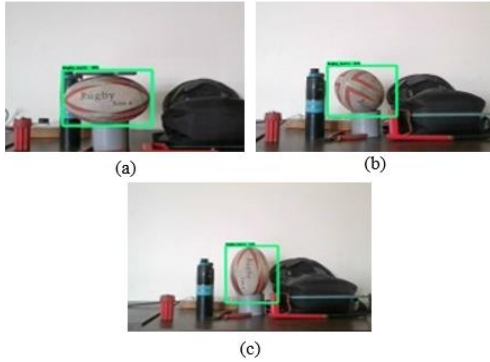


Fig. 10. Testing different orientations. (a) Horizontal, (b) Tilted, (c) Vertical.

## C. Performance of object tracking

The performance of object tracking highly depends on the computational cost to run the algorithm for each frame. The size of the object detection model directly affects the Frames per Second (FPS) by increasing the computational cost. The performance of the object tracking algorithm was evaluated based on the FPS procured and the size of the model. To compare, the base model trained on SSD MobileNet was quantized using an 8-bit quantizer. The results are compared in the table below.

TABLE I. COMPARISON BETWEEN THE BASE AND QUANTIZED MODEL.

Model	FPS	Accuracy	Model Size
SSD MobileNet	2.43	0.984	35.47 Mb
SSD MobileNet 8-bit Quantized	5.86	0.950	8.44 Mb

## VI. CONCLUSION

The paper presents a simple yet robust object tracking system using CNN based framework for object recognition. The method regulates the tracking of the object with variable speed in the frame to re-center it to the origin. Based on a custom dataset of a rugby ball, the system is tested for mobile compatibility of the model using SSD MobileNet as well as its quantized version. The results are compared on the metrics of FPS, accuracy, and size of the model to test its compatibility on Raspberry Pi 4B. Moreover, the quantized model was tested along with a vision system on a holonomic system to examine the responsiveness of the object tracking algorithm towards the variable speed of the object in the frame. The methods used in the paper can be used to develop a quick and responsive maneuvering mechanism for robotic systems. Also, the work in

the paper can be utilized to develop a robust yet minuscule model compatible with embedded systems.

## REFERENCES

- [1] Pathak AR, Pandey M, Rautaray S. Application of deep learning for object detection. *Procedia computer science*. 2018 Jan 1;132:1706-17.
- [2] Zou Z, Shi Z, Guo Y, Ye J. Object detection in 20 years: A survey. *arXiv preprint arXiv:1905.05055*. 2019 May 13.
- [3] Wu, Yi, Jongwoo Lim, and Ming-Hsuan Yang. "Online object tracking: A benchmark." In *Proceedings of the IEEE conference on computer vision and pattern recognition*, pp. 2411-2418. 2013.
- [4] Allen, Peter K., Aleksandar Timcenko, Billibon Yoshimi, and Paul Michelman. "Automated tracking and grasping of a moving object with a robotic hand-eye system." *IEEE Transactions on Robotics and Automation* 9, no. 2 (1993): 152-165.
- [5] Vasconez, Juan Pablo, J. Delpiano, S. Vougioukas, and F. Auat Cheein. "Comparison of convolutional neural networks in fruit detection and counting: A comprehensive evaluation." *Computers and Electronics in Agriculture* 173 (2020): 105348.
- [6] Pin, Francois G., and Stephen M. Killough. "A new family of omnidirectional and holonomic wheeled platforms for mobile robots." *IEEE transactions on robotics and automation* 10, no. 4 (1994): 480-489.
- [7] Holmberg, Robert, and Oussama Khatib. "Development and control of a holonomic mobile robot for mobile manipulation tasks." *The International Journal of Robotics Research* 19, no. 11 (2000): 1066-1074.
- [8] Bo, Liefeng, Xiaofeng Ren, and Dieter Fox. "Unsupervised feature learning for RGB-D based object recognition." In *Experimental robotics*, pp. 387-402. Springer, Heidelberg, 2013.
- [9] Jafari, Omid Hosseini, Dennis Mitzel, and Bastian Leibe. "Real-time RGB-D based people detection and tracking for mobile robots and head-worn cameras." In *2014 IEEE international conference on robotics and automation (ICRA)*, pp. 5636-5643. IEEE, 2014.
- [10] Parhi, Dayal R. "Navigation of mobile robots using a fuzzy logic controller." *Journal of intelligent and robotic systems* 42, no. 3 (2005): 253-273.
- [11] Yilmaz, Alper, Omar Javed, and Mubarak Shah. "Object tracking: A survey." *Acm computing surveys (CSUR)* 38, no. 4 (2006): 13-es.
- [12] Leibe, Bastian, Aleš Leonardis, and Bernt Schiele. "Robust object detection with interleaved categorization and segmentation." *International journal of computer vision* 77, no. 1 (2008): 259-289.
- [13] Kang, Kai, Hongsheng Li, Junjie Yan, Xingyu Zeng, Bin Yang, Tong Xiao, Cong Zhang et al. "T-cnn: Tubelets with convolutional neural networks for object detection from videos." *IEEE Transactions on Circuits and Systems for Video Technology* 28, no. 10 (2017): 2896-2907.
- [14] Tusch, Anne-Marie, Stéphane Herbin, and Jean-Yves Audibert. "Semantic hierarchies for image annotation: A survey." *Pattern Recognition* 45, no. 1 (2012): 333-345.
- [15] Mottaghi, Roozbeh, Xianjie Chen, Xiaobai Liu, Nam-Gyu Cho, Seong-Whan Lee, Sanja Fidler, Raquel Urtasun, and Alan Yuille. "The role of context for object detection and semantic segmentation in the wild." In *Proceedings of the IEEE Conference on Computer Vision and Pattern Recognition*, pp. 891-898. 2014.
- [16] Tellez, David, Geert Litjens, Péter Bánci, Wouter Bulten, John-Melle Bokhorst, Francesco Ciompi, and Jeroen van der Laak. "Quantifying the effects of data augmentation and stain color normalization in convolutional neural networks for computational pathology." *Medical image analysis* 58 (2019): 101544.
- [17] Howard, Andrew G., Menglong Zhu, Bo Chen, Dmitry Kalenichenko, Weijun Wang, Tobias Weyand, Marco Andreetto, and Hartwig Adam. "Mobilenets: Efficient convolutional neural networks for mobile vision applications." *arXiv preprint arXiv:1704.04861* (2017).
- [18] Liu, Wei, Dragomir Anguelov, Dumitru Erhan, Christian Szegedy, Scott Reed, Cheng-Yang Fu, and Alexander C. Berg. "Ssd: Single shot multibox detector." In *European conference on computer vision*, pp. 21-37. Springer, Cham, 2016.

# Effective Object Detection and Tracking for Holonomic Robot using Deep Neural Architecture

Atharva V. Pawar  
Computer Engineering Dept.  
Saffrony Institute of Technology  
Mehsana, India  
atharva.vijay.pawar@gmail.com

Sejal J. Rajput  
Computer Engineering Dept.  
Saffrony Institute of Technology  
Mehsana, India  
sejalrajput@gmail.com

Hima K. Soni  
Computer Engineering Dept.  
Saffrony Institute of Technology  
Mehsana, India  
hima.soni@saffrony.ac.in

Nirav R. Joshi  
Electrical Engineering Dept.  
Saffrony Institute of Technology  
Mehsana, India  
nirav.joshi@saffrony.ac.in

**Abstract**—The power of Deep Learning-based Computer Vision is not only making Object Detection tasks efficient but also more interesting. It gives an ability to computers for performing complex tasks as humans by locating and distinguishing between objects. The present research paper aims to create a robust tracking algorithm based on a custom-built dataset of a rugby ball, generated to replicate industrial objects. With the rapid growth in the automation industry, the need for compact yet reliable computational algorithms is a necessity. The primary objective behind the whole system is to achieve mobile compatibility with accurate object detection and tracking. The work also states the usage of the Convolutional Neural Networks (CNN) to increase the overall performance of pattern/image detection in tracking problems. A simple yet robust object tracking algorithm accompanied with object detection on Single Shot Multi-Box Detector (SSD) MobileNet architecture is applied in this paper. The method offers a minuscule model compatible to run on embedded systems without trading off much performance.

**Keywords**—Object Detection, Object Tracking, Holonomic Robot, Automation, Embedded System, Computer Vision

## I. INTRODUCTION

Object detection is an inextricable part of the modern field of computer vision [1]. The ability of computers to perform complex tasks to locate and distinguish between objects has disrupted the conventional method to pave the path towards the industrial revolution [2]. Defense, automobile, and security & surveillance are few among the many industries disrupted by advances in the field of object detection. Object tracking deals with estimating the trajectory of the object in a confined image plane [3]. A tracking algorithm uses object-centric information such as shape, color, bound area, and orientation of the object. Though an efficacious method to solve complex real-time problems, complex object shapes, inefficient 3D to the 2D projection of objects, noisy image, and real-time computational cost are hurdles for object tracking.

Autonomous systems in [4],[5] show the potential of combined systems to execute the tasks with human-like precision and if not, more. The amalgamation of object detection, object tracking, vision systems, and superior robotic maneuvering has led to more reliable systems. References [6],[7] outperforms the conventional drive of non-holonomy with the holonomic drive approach. Having a controllable degree of freedom equivalent to the total degree of freedom, the

holonomic drive is commonly used in several mobile robots to perform autonomous as well as semi-autonomous tasks.

Convolutional Neural Networks (CNN) offers excellent overall performance in pattern/image detection, surpassing human beings. Recent advances in CNN algorithms have opened new state-of-the-art techniques for image classification, object detection, object tracking, and semantic segmentation. Hierarchical feature representation has led to an increase in expressive capability and joint optimization [8], which surpasses the capabilities of traditional methods.

Various mobile robots were studied in [9],[10] dealing with, robot navigation, obstacle avoidance, and accelerated object tracking methods. The mobile robots had common characteristics of non-holonomic drive and constructed a framework based on CNN, fuzzy logic, image processing, or monocular vision feedback. The non-holonomic drive in the study showed less freedom for robust tracking of an object in the 2D plane, lacking in the continuous and proportional relationship between the speed of the object to be tracked with the speed of the robot.

Considering the scope of improvements in conventional methods of object tracking, a robust yet simple logical algorithm based on CNN to detect an object using the centroid of the bounding box is applied in this paper. The method offers a robust algorithm with freedom of locomotion on a horizontal plane with dynamic speed monitoring of the robot to locate, track, and follow. Also, the approach is tested on a holonomic robot accompanied with Omni wheels-based drive to evaluate the motion on the horizontal plane. The mechanical structure is monitored by an object detection model to detect rugby balls, trained on SSD MobileNet. This replicates the industrial application of tracking complicated objects. Also, providing a robust yet compact model to run on embedded systems.

## II. GENERIC OBJECT DETECTION AND TRACKING

Recent frameworks of object detection algorithms permit object classification and position estimation of detected objects. Moreover, the development of frameworks in [11],[12] overcome complexity such as occlusions, noisy images, information lost due to projection of environment into a 2D image, complex shapes of objects, and real-time computational requirements. These advances have helped make modern-day object detection algorithms more robust than ever.

In general object detection, once the object is detected, the tracking algorithm estimates the trajectory of the object through instance-by-instance evaluation of the frame in the video.

A flow and various approaches for object detection and tracking are demonstrated in Fig. 1.

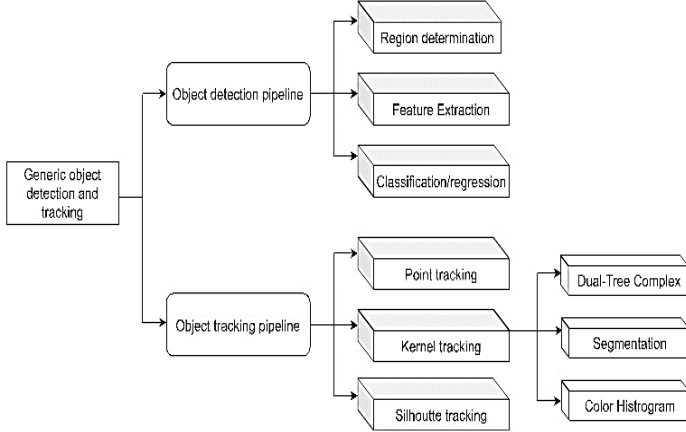


Fig. 1. Various object detection and tracking approaches

### A. Object detection pipeline

To determine the location of object (Object localization) and category of the detected object (Object classification), the pipeline of the object detection approach is divided into three stages which are further discussed below.

1) *Region determination*: Different classes of objects at multiple positions, different aspect ratios and sizes governs the computational expenses of the algorithm. Sliding multi-scale windows on images are observed to be an obvious yet exhaustive and inefficient method to locate the region of interest (ROI). Furthermore, work in [13] showcases the ability to mimic the human brain up to some extent for scanning and focusing on ROI by utilizing CNN into sliding window to directly predict the top-most feature (CNN layer) by bounding boxes after obtaining the confidence of the object class.

2) *Feature extraction*: To extract visual features, methods like segmentation, robust representation, and recognizing different classes are essential. These features are extracted from high dimensional features to final representation using CNN in a fixed resolution of the proposed region in the frame.

3) *Classification/ Regression*: Unique identification of the specific object's class is a vital parameter for the evaluation of models' robustness. More hierarchical, semantic, and informative visual recognitions presented using the classifier in [14] resulted in better clustering of classes. Utilizing CNN, allows the training of models to learn key representations without the need to design the features manually. The weights and biases in the network established are frozen to extract the best-performing model. Finally, different determined regions are scored on the set of positive regions (ROI) and negative regions (i.e., background). Bounding box regressors are then fit on the scored regions to extract the final location of the object.

### B. Object tracking pipeline

Continuous path estimation of the object in motion in the instance is the primary task of the object tracking algorithm. The target object is traced by selecting accurate features and object representations. In the first stage, optical flow, contours-based and histogram-based representation, and features recognized by CNN are some of the most common methods for feature detection. In the second stage, these feature detectors are utilized to create a correspondence between object occurrence in the frame both separately and jointly. Object tracking methods can be broadly categorized into three parts as discussed below.

1) *Point tracking*: The correspondence of detected objects is represented by points across the frames in point tracking. These points are identified using deterministic and statistical methods. Generic thresholding is done using point recognition. Moreover, occasions and false detections are shortcomings for the method.

2) *Kernel tracking*: Potential regions of objects are represented frame by frame for computing the object in motion. Parametric motions such as affined, conformal, and translational are observed. Usually, different types of objects are tracked, and approximating the motion of the object is done. Few kernel-based tracking approaches are:

a) *Dual-Tree Complex Wavelet Transform Technique*: Real wavelet transform employed here leads to poor directionality & shift variance and complex wavelet transform. Real filters are used to obtain shift variance in the tracking technique.

b) *Segmentation*: The approach finds the object in motion through optical flow computation. A considerable part of the video sequence is converted into gray-scale to apply the Horn-Schunk method for optical flow determination between any two images. The magnitude squared values of the optical flow,  $|V|^2$ , is calculated to compare the mean value of the first image with the optical flow of each pixel in the frame of the video sequence. Pixel values for each image are then set as true or high if  $|V|^2$ , at any pixel, is greater than or equal to the mean.

c) *Object tracking using Color Histogram*: Target model and candidate models are established in feature space to characterize the model. As illustrated in (1), the target model is defined as a probability density function  $\hat{q}$  in the given feature space. Similarly, the candidate model is defined as  $y$  and also characterized as the probability density function  $\hat{p}(y)$ . Further, a similarity function  $\hat{p}(y)$ , Bhattacharyya coefficient between  $\hat{p}$  and  $\hat{q}$  play the role of the likelihood for the local maxima in the frame indicating the presence of the object.

$$d(y) = \sqrt{1 - \rho[\hat{p}(y), \hat{q}]} \quad (1)$$

3) *Silhouette tracking*: Many times objects have complex shapes which cannot be fit geometrically in the object tracking mechanism, a silhouette-based approach is used to bound the detected objects in descriptive shapes. The method can represent in the form of edges, histogram, and contours. The silhouette tracking method can be classified into two categories, shape matching, and contour tracking.

### III. OBJECT DETECTION AND TRACKING USING ITERATIVE RE-CENTRING APPROACH

A robotic system was designed to implement the task of object detection and object tracking to capture the ball in motion with live feedback from vision systems.

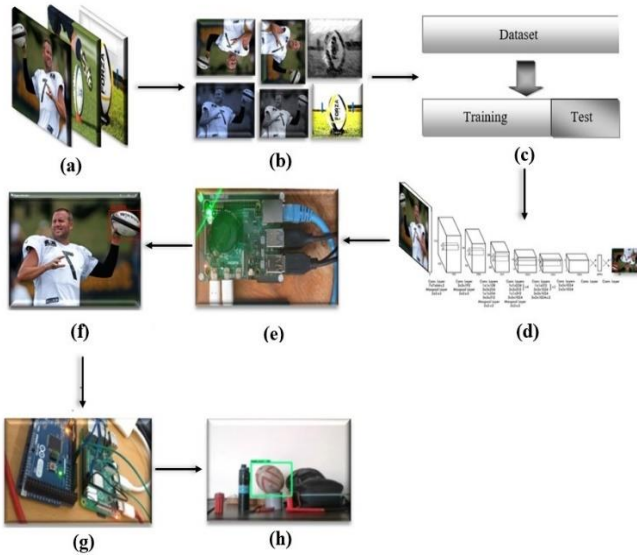


Fig. 2 (a) Gathering Images, (b) Augmentation, (c) Splitting Data, (d) Training of model, (e) Deploy on Raspberry Pi, (f) Run the model with bounding box and get coordinates, (g) Send coordinates to Arduino, (h) Track the ball.

To recognize the rugby ball distinctly, an object detection algorithm SSD MobileNet was utilized. The generated model by the algorithm being compact in terms of model size and computational power to run makes it feasible to accommodate it on an embedded system for the task of object detection. The steps performed and applied algorithms are demonstrated below:

#### A. Dataset

In object detection, images play a crucial role for a model to learn from and act as a source to gather salient features [15]. A total of 3300 sample images of rugby balls were collected in various orientations, backgrounds, colors, and angles. Such variance in sample images provides a generalized input for real possible scenarios while detection. Moreover, a close examination of the dataset was done to generate the same proportion of images with different characteristics to avoid undesirable bias for the model training.

The major portion of the dataset was gathered by employing the web-scraping algorithm to extract images of rugby balls effortlessly. The dataset also consisted of snaps of a rugby ball in different orientations, lighting conditions, and occlusions which were gathered locally. Finally, as shown in Fig. 2(a) all the images were resized to 300 X 300-pixel dimensions for equal scaling of all the data points.

#### B. Data augmentation and labeling

Due to the lack of ample amount of data points as well as the diversity of the data, inefficient extraction of salient features can be induced, resulting in underperformance of the model [16]. Data augmentation techniques applied on datapoints can

aid in scaling the dataset by folds and allows attaining the generalization by adding diversity to the data points. Data augmentation techniques such as interpolation, color distortion, blur, noise injection, cropping, flip, and rotations were applied as shown in Fig. 2(b).

The collected data points were split into training and testing data and annotated to provide the pivotal metadata for the supervised training of the model. Annotations are important features for determining the location and pixel area covered by the object in the image. Which helps in feature extraction while training, restricting computation to the ROI, and assists in robust modeling of the data points.

#### C. Model architecture and training

The images of the dataset were fine-tuned on a pre-trained neural architecture using the SSD algorithm, SSD MobileNet. The algorithm performs the tasks of object localization & classification, bounding box regression, and a classifier network to distinguish the detected objects. The architecture accompanies two deep neural networks, a base network (MobileNet) and a detection network (SSD). The base network can be divided into two blocks, depth-wise separable convolution ( $D_w$ ) and point-wise convolution ( $P_w$ ) [17].

*a) Depth-wise separable layer:* Depth-wise layer is utilized for filtering while the point-wise layer is utilized for combining the incoming feature maps from various channels. A standard convolutional layer consists of  $D_K \times D_K \times D_K$  input [17],  $M$  being the input channels through  $N$  convolution kernels for  $N$  feature maps for kernel size  $K$ . The standard computational cost can be calculated as in (2).

$$D_K \cdot D_K \cdot M \cdot N \cdot D_F \cdot D_F \quad (2)$$

$$D_K \cdot D_K \cdot M \cdot D_F + M \cdot N \cdot D_F \cdot D_F \quad (3)$$

Since a depth-wise separable convolution consists of depth-wise convolution and a point-wise convolution. The total computational cost is shown in (3). The computing ratio of depth-wise separable convolution and standard convolutions is expressed in (4).

$$\frac{D_K \cdot D_K \cdot M \cdot D_F \cdot D_F + M \cdot N \cdot D_F \cdot D_F}{D_K \cdot D_K \cdot M \cdot N \cdot D_F \cdot D_F} \quad (4)$$

A drastic decrement in the computation cost of depth-wise separable convolution can be learned in (5) [17].

$$\frac{1}{N} + \frac{1}{D_K^2} \quad (5)$$

*b) Inverted residuals:* The vulnerability of information loss increases after ReLU operation on lower-dimensional features in depth-wise separable convolution. The linear bottleneck is a complement to the depth-wise separable convolution. ReLU is replaced by a linear activation function to avoid further information losses. Point-wise convolution is used to advance the dimension to increase the channels after depth-wise processing.

*c) Single Shot MultiBox Detector (SSD):* The detection network is a single feed-forward-based convolutional neural

network capable of multi-target detection by simultaneously predicting the target categories with bounding boxes [18]. SSD is built on venerable VGG-16 architecture with six auxiliary feature layers, delivering strong performance in high-quality image classification and its ability to implement transfer learning to improve results. To predict the different types of offsets of the boxes with different scales, aspect ratios, and corresponding confidences, large amounts of multi-scaled borders are generated at different information layers. A fast class-agnostic bounding box co-ordinates proposal method is used for bounding box regression. The method uses a 1 X 1 convolution for dimensionality reductions but preserves the width and height. As in (6), the cumulative multi-box loss function is governed by confidence loss and location loss.

$$\text{multibox loss} = \text{confidence loss} + \alpha \times \text{location loss} \quad (6)$$

#### D. Tracking Algorithm

To track and maneuver the mechanism for rugby ball and get repeated feedback of the object in the environment through a vision system, a tracking algorithm was employed. The algorithm comes next in the pipeline after object detection in the frame as shown in Fig. 2(h). The frame is split into four quadrants and scaled for the input frame dimension of 480 X 360, resulting in diminishing the computational cost for frame evaluation. Moreover, the algorithm provides a tracking approach for the variable speed of the object in the frame. The centroid-focused tracking algorithm is divided into parts and explained:

a) *Generate bounding boxes*: The object in the frame is detected by the trained model. To generate the location of the detected rugby ball in the frame, rectangular bounding boxes are formed to enclose the target. Enabling accurate positioning of the rugby ball in the frame and aids in extracting the coordinates of the enclosed area in the rectangular space. The boxes can be generated in any quadrant of the frame leading to consistent locating.

b) *Generate centroid*: Though the bounding boxes can produce the accurate area of the rugby ball in the frame, they fail to extract the location of the object at point precision. Centroid-based tracking can solve the problem by calculating the centroid of the rectangular bounding box used to enclose the rugby ball for points  $M_{00}$ ,  $M_{01}$ ,  $M_{10}$ ,  $M_{11}$  as demonstrated in (7). Resulting in an average location of the detected object, returning a point on the X-Y plane. Diminishing the ROI into point of interest (POI), the task of precisely locating the object can be accomplished.

$$\frac{M_{00} + M_{01} + M_{10} + M_{11}}{4} \quad (7)$$

c) *Co-ordinate mapping and re-centering*: To track the motion of a rugby ball horizontally using an iterative re-centering mechanism, co-ordinate mapping is introduced. With the rugby ball in motion with variable velocity, the system can fail due to slow reaction time. Analog mapping of horizontal coordinates is implemented to assign variable speed for the horizontal re-centering of the robotic base. The positioning is monitored using iterative feedback from the vision system.

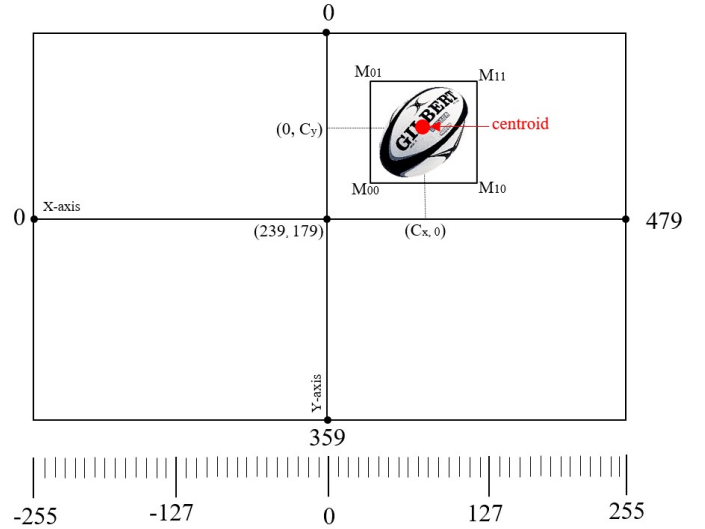


Fig. 3 Visualization of co-ordinate mapping and recentering

The base of the holonomic robot is dynamically re-centered for speed-sensitive to the horizontal coordinates of the detected centroid. The visualization of the iterative algorithm as depicted in Fig. 3 monitors in a simple yet robust manner and dynamically vary the velocity for tracking as well as re-centering the rugby ball.

#### IV. EXPERIMENTAL SETUP

The trained SSD MobileNet model and proposed object tracking method were tested on the holonomic structure shown in Fig. 4. The system includes four Omni-wheels coupled with planetary gear motors at the base providing smooth locomotion on a horizontal plane. This allows a degree of freedom for two axes. The structure incorporates a vision system, computational boards: Raspberry Pi, Arduino Mega, Motor Drivers to synchronize the motion of motors, and Communication Bus Architecture to regulate the transferring of information between computational boards. The system is powered by a 12V LiPo battery. Which supplies power to motor drivers, synchronizing the motors. The actions of these motor drivers are regulated by Arduino Mega assisted by logical conditions applied in Arduino sketch.

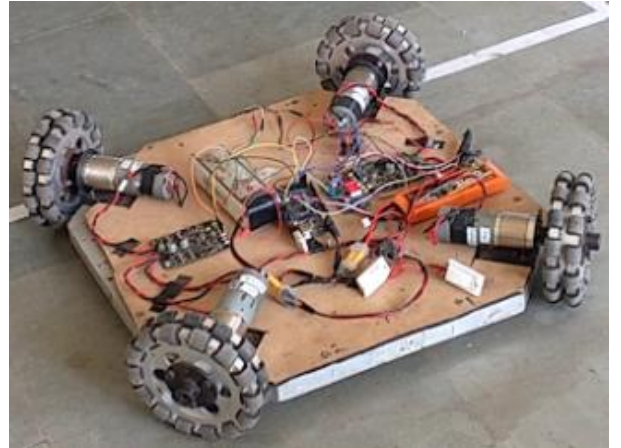


Fig. 4. Holonomic Structure

The camera module in connection with Raspberry Pi 4B with 4GB RAM and quad-core A72 cortex processor, captures the frames in the live feed. The captured frame is monitored to detect the rugby ball with bounding boxes. The coordinates of the detected bounding boxes are utilized to calculate centroid points and transferred to the Arduino Mega using the I2C communication protocol. The base of the robot is re-centered sensitively using analog-based velocity mapping under the monitoring of logical parameters by Arduino. The system was tested in multiple environments.

## V. RESULTS AND DISCUSSION

The paper presents the results of the validation of the rugby ball dataset. The dataset was split into a split ratio of 0.8 and 0.2 for the training and validation of the model, respectively. The model was trained up to 25100 iterations. For the overall evaluation of our approach, several evaluation metrics were performed to study the results.

### A. Evaluation of training performance

For detection of a rugby ball, the SSD MobileNet was fine-tuned on the custom dataset. The training session was conducted on Tesla K80 GPU with 12GB RAM. Based on the training session, various observations have been done using TensorBoard with step and their respective losses on the x-axis and y-axis respectively as shown in Fig. (5)-(9).

To evaluate the accuracy of the prediction of classes by model, classification loss as shown in Fig. 5 was plotted. With an increment in the number of steps, the losses decreased constantly till 0.2. This showcases the robust classification ability of the trained model.

The localization loss as shown in Fig. 7 was visualized to evaluate the error between predicted bounding box corrections and true values. The results show minimal losses due to localization resulting in a reduction of loss to 0.1. Moreover, Normalized loss in Fig. 7, as well as regularization loss in Fig. 8, were reduced below 0.5 and 0.2, respectively. This demonstrates the generalization property of the model, leading towards better accuracy.

Finally, the total loss in Fig. 9 was a plot for evaluating the overall loss in terms of classification, regularization, and localization. Total loss constantly decreased up to 0.5.

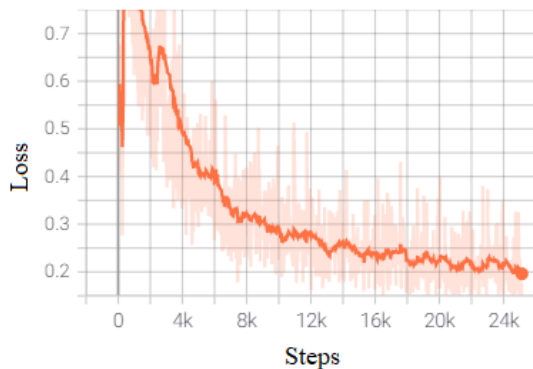


Fig. 5. Classification Loss

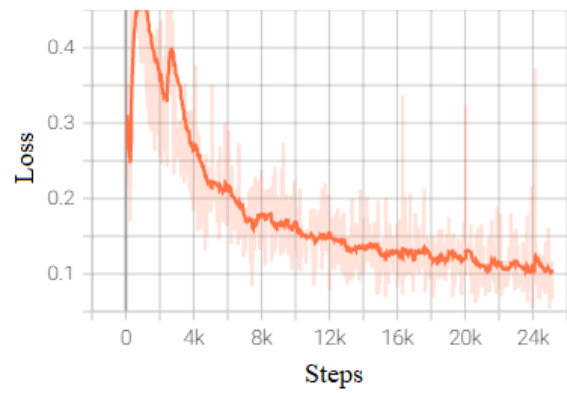


Fig. 6. Localization Loss

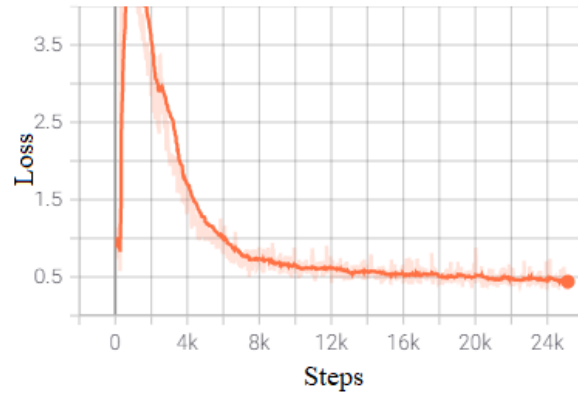


Fig. 7. Normalized Loss

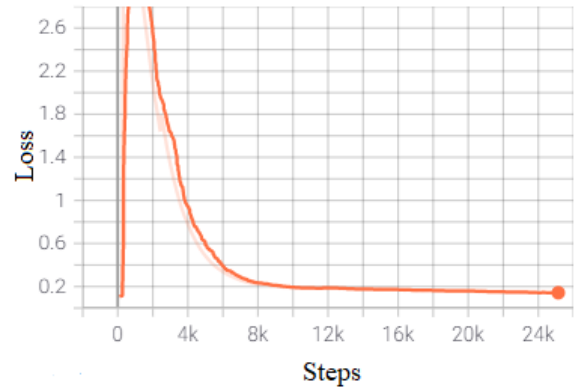


Fig. 8. Regularization Loss

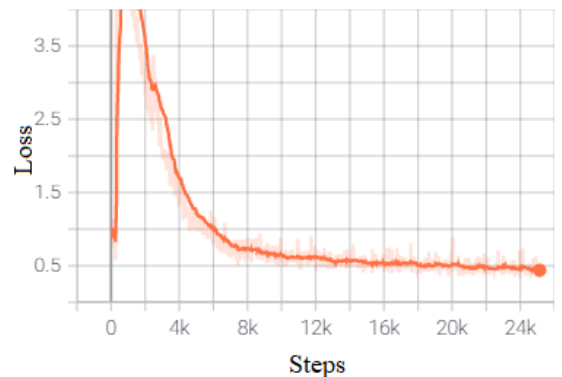


Fig. 9. Total Loss

## B. Object detection in action

After model training and studying the graphs, a minuscule model was tested to detect the rugby ball in various robust environments along with multiple objects in the surroundings. Moreover, to test the reliability of the generalization of the trained model, the rugby ball was adjusted at different orientations. As seen in Fig. 10 the model was able to detect the location of the rugby ball at different orientations and could distinguish between different objects.

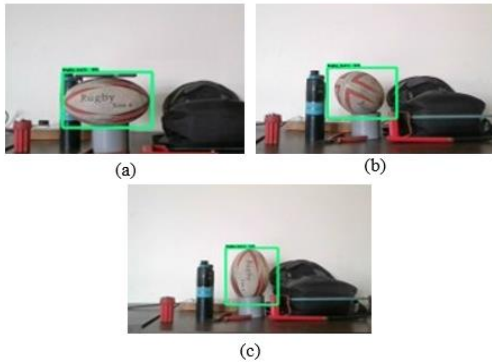


Fig. 10. Testing different orientations. (a) Horizontal, (b) Tilted, (c) Vertical.

## C. Performance of object tracking

The performance of object tracking highly depends on the computational cost to run the algorithm for each frame. The size of the object detection model directly affects the Frames per Second (FPS) by increasing the computational cost. The performance of the object tracking algorithm was evaluated based on the FPS procured and the size of the model. To compare, the base model trained on SSD MobileNet was quantized using an 8-bit quantizer. The results are compared in the table below.

TABLE I. COMPARISON BETWEEN THE BASE AND QUANTIZED MODEL.

Model	FPS	Accuracy	Model Size
SSD MobileNet	2.43	0.984	35.47 Mb
SSD MobileNet 8-bit Quantized	5.86	0.950	8.44 Mb

## VI. CONCLUSION

The paper presents a simple yet robust object tracking system using CNN based framework for object recognition. The method regulates the tracking of the object with variable speed in the frame to re-center it to the origin. Based on a custom dataset of a rugby ball, the system is tested for mobile compatibility of the model using SSD MobileNet as well as its quantized version. The results are compared on the metrics of FPS, accuracy, and size of the model to test its compatibility on Raspberry Pi 4B. Moreover, the quantized model was tested along with a vision system on a holonomic system to examine the responsiveness of the object tracking algorithm towards the variable speed of the object in the frame. The methods used in the paper can be used to develop a quick and responsive maneuvering mechanism for robotic systems. Also, the work in

the paper can be utilized to develop a robust yet minuscule model compatible with embedded systems.

## REFERENCES

- [1] Pathak AR, Pandey M, Rautaray S. Application of deep learning for object detection. *Procedia computer science*. 2018 Jan 1;132:1706-17.
- [2] Zou Z, Shi Z, Guo Y, Ye J. Object detection in 20 years: A survey. *arXiv preprint arXiv:1905.05055*. 2019 May 13.
- [3] Wu, Yi, Jongwoo Lim, and Ming-Hsuan Yang. "Online object tracking: A benchmark." In *Proceedings of the IEEE conference on computer vision and pattern recognition*, pp. 2411-2418. 2013.
- [4] Allen, Peter K., Aleksandar Timcenko, Billibon Yoshimi, and Paul Michelman. "Automated tracking and grasping of a moving object with a robotic hand-eye system." *IEEE Transactions on Robotics and Automation* 9, no. 2 (1993): 152-165.
- [5] Vasconez, Juan Pablo, J. Delpiano, S. Vougioukas, and F. Auat Cheein. "Comparison of convolutional neural networks in fruit detection and counting: A comprehensive evaluation." *Computers and Electronics in Agriculture* 173 (2020): 105348.
- [6] Pin, Francois G., and Stephen M. Killough. "A new family of omnidirectional and holonomic wheeled platforms for mobile robots." *IEEE transactions on robotics and automation* 10, no. 4 (1994): 480-489.
- [7] Holmberg, Robert, and Oussama Khatib. "Development and control of a holonomic mobile robot for mobile manipulation tasks." *The International Journal of Robotics Research* 19, no. 11 (2000): 1066-1074.
- [8] Bo, Liefeng, Xiaofeng Ren, and Dieter Fox. "Unsupervised feature learning for RGB-D based object recognition." In *Experimental robotics*, pp. 387-402. Springer, Heidelberg, 2013.
- [9] Jafari, Omid Hosseini, Dennis Mitzel, and Bastian Leibe. "Real-time RGB-D based people detection and tracking for mobile robots and head-worn cameras." In *2014 IEEE international conference on robotics and automation (ICRA)*, pp. 5636-5643. IEEE, 2014.
- [10] Parhi, Dayal R. "Navigation of mobile robots using a fuzzy logic controller." *Journal of intelligent and robotic systems* 42, no. 3 (2005): 253-273.
- [11] Yilmaz, Alper, Omar Javed, and Mubarak Shah. "Object tracking: A survey." *Acm computing surveys (CSUR)* 38, no. 4 (2006): 13-es.
- [12] Leibe, Bastian, Aleš Leonardis, and Bernt Schiele. "Robust object detection with interleaved categorization and segmentation." *International journal of computer vision* 77, no. 1 (2008): 259-289.
- [13] Kang, Kai, Hongsheng Li, Junjie Yan, Xingyu Zeng, Bin Yang, Tong Xiao, Cong Zhang et al. "T-cnn: Tubelets with convolutional neural networks for object detection from videos." *IEEE Transactions on Circuits and Systems for Video Technology* 28, no. 10 (2017): 2896-2907.
- [14] Tusch, Anne-Marie, Stéphane Herbin, and Jean-Yves Audibert. "Semantic hierarchies for image annotation: A survey." *Pattern Recognition* 45, no. 1 (2012): 333-345.
- [15] Mottaghi, Roozbeh, Xianjie Chen, Xiaobai Liu, Nam-Gyu Cho, Seong-Whan Lee, Sanja Fidler, Raquel Urtasun, and Alan Yuille. "The role of context for object detection and semantic segmentation in the wild." In *Proceedings of the IEEE Conference on Computer Vision and Pattern Recognition*, pp. 891-898. 2014.
- [16] Tellez, David, Geert Litjens, Péter Bánci, Wouter Bulten, John-Melle Bokhorst, Francesco Ciompi, and Jeroen van der Laak. "Quantifying the effects of data augmentation and stain color normalization in convolutional neural networks for computational pathology." *Medical image analysis* 58 (2019): 101544.
- [17] Howard, Andrew G., Menglong Zhu, Bo Chen, Dmitry Kalenichenko, Weijun Wang, Tobias Weyand, Marco Andreetto, and Hartwig Adam. "Mobilenets: Efficient convolutional neural networks for mobile vision applications." *arXiv preprint arXiv:1704.04861* (2017).
- [18] Liu, Wei, Dragomir Anguelov, Dumitru Erhan, Christian Szegedy, Scott Reed, Cheng-Yang Fu, and Alexander C. Berg. "Ssd: Single shot multibox detector." In *European conference on computer vision*, pp. 21-37. Springer, Cham, 2016.